Check for updates

Human–climate–environment interactions in Espiritu Santo, Vanuatu during the past millennium

Giorgia Camperio [1,2]*, S. Nemiah Ladd [3],
Matiu Prebble [4,5,6], Cindy De Jonge [2],
Tobias Schneider [1], Elena Argiriadis [7,8],
Ronald Lloren [1,2], Daniel B. Nelson [9],
Amicie A. Delahaie [1,10], Christiane Krentscher[1] and
Nathalie Dubois [1,2]

[1]Department of Surface Waters Research and Management, Eawag, Dübendorf, Switzerland, [2]Geological Institute, Department of Earth Sciences, ETH Zürich, Zürich, Switzerland, [3]Department of Environmental Sciences, University of Basel, Basel, Switzerland, [4]School of Earth and Environment, College of Science, University of Canterbury, Christchurch, New Zealand, [5]Archaeology and Natural History, Culture History and Languages, The Australian National University, Canberra, ACT, Australia, [6]Te Punaha Matatini, University of Auckland, Auckland, New Zealand, [7]Institute of Polar Sciences, CNR-ISP, Venice, Italy, [8]Department of Environmental Sciences, Informatics and Statistics, Ca' Foscari University, Venice, Italy, [9]Department of Environmental Sciences − Botany, University of Basel, Basel, Switzerland, [10]Laboratory of Geology, École Normale Supérieure, CNRS, PSL University, IPSL, Paris, France

Over the past millennium, the tropical Pacific Islands of Remote Oceania have experienced significant transformations caused by different waves of human settlement and climatic variability. However, many sites remain to be explored for their archeological potential, and the complex climatic setting of the tropical Pacific further complicates our understanding of past environmental and societal changes. In this study, we applied a multi-proxy approach to sediment cores extracted from ponds on the west coast of Espiritu Santo, Vanuatu to investigate past human-climate-environment dynamics. Through the analysis of human-associated proxies including fecal markers, palmitone (a specific lipid biomarker for taro), crop pollen and sedimentary charcoal, we inferred changes in human presence and activities. We reconstructed past hydroclimate from leaf wax hydrogen isotopes ($\delta^2 H_{LW}$) and past temperatures from branched glycerol dialkyl glycerol tetraethers (brGDGTs). Changes in pollen reveal major shifts in local and regional vegetation. In our record, the period from 1000 to 1300 CE was characterized by warm/wet conditions concomitant with demographic expansion inland. Around 1400 CE, pollen, leaf wax distributions, and $\delta^2 H_{LW}$ data indicated a drier period. The coincident decrease in palmitone, despite high charcoal and fecal marker concentrations, suggested that drier conditions might have rapidly restricted taro cultivation, but not the overall population, which declined more than a century later. We hypothesize that the establishment of one of the earliest European settlements in Oceania in 1606 CE further disrupted local demographics with the introduction of epidemic diseases. This study contributes to our understanding of the intricate relationship between human activities, climatic

fluctuations, and landscape modifications in Remote Oceania over the past millennium.

1 Introduction

Human activities have been a driving force in shaping island ecosystems since the arrival of the first settlers (Nogué et al., 2021). The oceanic islands of the Pacific are some of the last places colonized by humans, and climatic shifts have exerted significant influence on past human settlement patterns and activities (Anderson et al., 2006; Allen, 2006; Montenegro et al., 2016; Sear et al., 2020). Furthermore, subsequent waves of human settlement, including initial indigenous settlement (Bedford and Spriggs, 2008), and later European colonization (Flexner, 2014), have contributed differently to the pattern of environmental transformation. Understanding the dynamic interplay between different waves of human settlement and climate change is crucial in light of ongoing environmental crises as it can provide knowledge to guide sustainable land-use strategies on island ecosystems (Nogué et al., 2017).

Remote Oceania encompasses islands and island societies known for their diverse cultures, languages, and landscapes (Green, 1991). Vanuatu is known for its remarkable linguistic diversity, which attests to its cultural and historical complexity (François et al., 2015). Settlement patterns over the last 1000 years contributed to the cultural-linguistic diversity observed today on the islands (Bedford and Spriggs, 2008), while land use practices, rooted in the culture of Vanuatu, have modified the landscape through activities including high intensity wetland cultivation (Bedford et al., 2018). Taro [*Colocasia esculenta* (L.) Schott], for example, is the main staple crop of the region and an integral part of the cultural landscapes of Vanuatu. Evidence of taro cultivation in irrigated gardens dates back to the last millennium (Spriggs, 1997b). Horticulture, particularly irrigated gardens as observed in Vanuatu over the past millennium (Bedford et al., 2018), is closely linked to environmental changes, including shifts in precipitation patterns (Camperio et al., 2024). However, the specific ways in which past climatic factors influence the livelihoods of islanders in these regions and the long-term impacts on food security, sustainability, and adaptation strategies remain uncertain. The complexity of climatic drivers in the Pacific coupled with the paucity of climatic records limits our understanding of regional climate variability and their effects on past human societies.
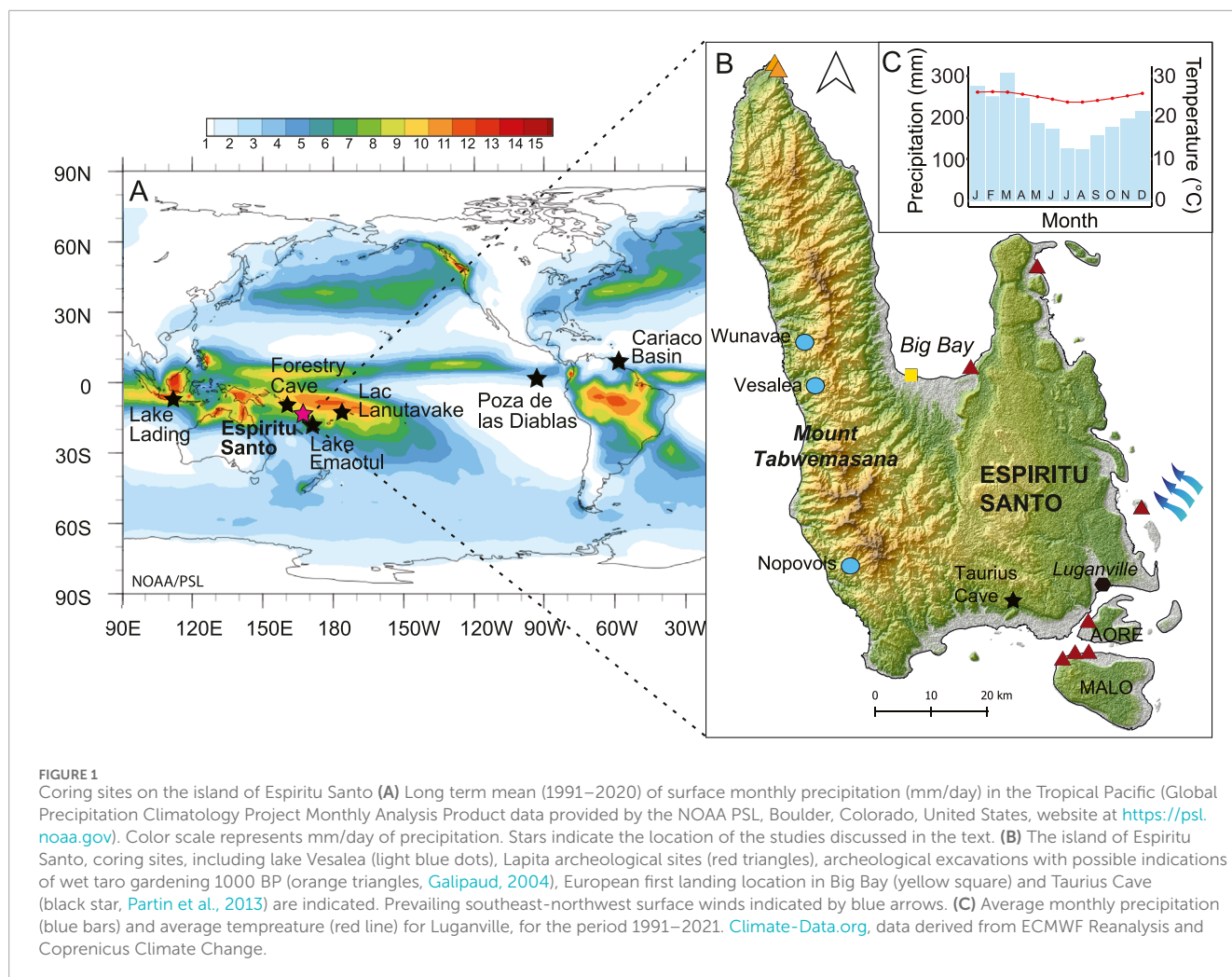
In Vanuatu, the South Pacific convergence Zone (SPCZ) is the main climatic driver of seasonal hydroclimatic variability (Maes and Varillon, 2011; Brown et al., 2020). It retracts to the north of its mean position in austral midwinter and extends southward of its mean position in austral midsummer changing in length and width. Long term shifts in the position of the SPCZ can result in dramatic changes in precipitation, impacting small South Pacific island communities (Brown et al., 2020). In contrast, interannual climatic variability in the Tropical Pacific is dominated by the El Niño–Southern Oscillation (ENSO) (Kilbourne et al., 2004), while on decadal to multidecadal timescales, the Interdecadal Pacific Oscillation (IPO) modulates ENSO teleconnections within the SPCZ region,

influencing precipitation patterns and extremes (Salinger et al., 2001). During El Niño events the islands in Vanuatu experience warmer and drier conditions often leading to droughts, while during La Niña wetter conditions lead to increased risk of flooding. The interaction between ENSO variability and other climatic features in the Tropical Pacific complicates our ability to understand the causes of past climatic change in this area, which has exhibited substantial variability over the past millennium with sometimes large regional differences (Brown et al., 2020; Atwood et al., 2021). In particular, contrasting hypotheses have been put forward for the hydroclimate of the Little Ice Age (LIA, ~1450–1850), such as a large-scale southward shift of the Intertropical Convergence Zone (ITCZ), a strengthened Pacific Walker Circulation, and/or an equatorward contraction of the monsoonal Asian-Australian rain belt (Atwood et al., 2021). Reconstructing these climate variations is crucial to understand their potential influence on past human populations in the Pacific region.

Here, we use sedimentological records from two ponds located on the west coast of Espiritu Santo (hereafter referred to as Santo), the largest island in Vanuatu, to reconstruct landscape modifications and disentangle the human and climatic factors that influenced the region over the last millennium (Figure 1). By studying changes in sediment composition, we infer shifts in climate, vegetation, land use practices, and other environmental factors that occurred in the catchment. We use fecal fossil molecules, namely coprostanol and its epimer, epicoprostanol, coupled with charcoal concentrations and crop pollen, as indicators of human presence and demographic changes (White et al., 2019; Keenan et al., 2021; Raposeiro et al., 2021). Charcoal concentrations and palmitone, a unique marker for the staple crop taro (Krentscher et al., 2019; Camperio et al., 2024), are used to track horticulture practices. Indicators of human presence and of human activities together are considered human traces. Branched glycerol dialkyl glycerol tetraether (brGDGTs) and the hydrogen isotopic composition of leaf waxes (δ^2H_{LW}) are used for climatic reconstructions (respectively for temperature and hydroclimate) (Sachse et al., 2012; De Jonge et al., 2014; Ladd et al., 2021), and palynology is established to track vegetational changes (Pickett et al., 2004). Finally, we reconstruct downcore changes in aquatic productivity and erosive events based on the total organic carbon content (TOC), carbon-to-nitrogen (C/N) ratio, biogenic silica and grain size distribution.

1.1 Environmental setting

Santo, the largest island of the Vanuatu archipelago, is geologically separated into two halves; the Sakao Peninsula in the East is made of terraced limestone from old coral reefs while the western side is dominated by the Cumberland Chain. This rapidly rising range of high volcanic mountains is oriented N-S and features steep slopes, ridges and deep valleys. Santo's Mount

FIGURE 1
Coring sites on the island of Espiritu Santo **(A)** Long term mean (1991–2020) of surface monthly precipitation (mm/day) in the Tropical Pacific (Global Precipitation Climatology Project Monthly Analysis Product data provided by the NOAA PSL, Boulder, Colorado, United States, website at https://psl. noaa.gov). Color scale represents mm/day of precipitation. Stars indicate the location of the studies discussed in the text. **(B)** The island of Espiritu Santo, coring sites, including lake Vesalea (light blue dots), Lapita archeological sites (red triangles), archeological excavations with possible indications of wet taro gardening 1000 BP (orange triangles, Galipaud, 2004), European first landing location in Big Bay (yellow square) and Taurius Cave (black star, Partin et al., 2013) are indicated. Prevailing southeast-northwest surface winds indicated by blue arrows. **(C)** Average monthly precipitation (blue bars) and average tempreature (red line) for Luganville, for the period 1991–2021. Climate-Data.org, data derived from ECMWF Reanalysis and Coprenicus Climate Change.

Tabwemasana is the highest peak of the archipelago, reaching 1,879 m a.s.l. (Tzerikiantz, 2006; Pineda, 2011). The location of Santo close to the boundary of the Australian and the Pacific plates causes high levels of seismic activity, with the highest uplift rates (between 2 mm/yr and 6 mm/yr) observed in the west coast (Jouannic et al., 1980; Gaven et al., 1980; Taylor, 1992). Uplifted terraces can be found along many parts of the coastline. The west coast of Santo is characterized by a drier climate compared to the rest of the island (Terry, 2011), which results from an orographic effect on the eastern flank due to the prevailing south-east winds hitting the high mountain chain. Many rivers on the west coast are small and intermittent during the dry season (July-October). In these drier conditions, taro is cultivated in terraces and irrigated by channeling part of a stream. Taro is still cultivated extensively with traditional techniques, although coconut plantations, established in the post-colonial period for copra, are also widespread.

The west coast of Santo is characterized by three main primary forest vegetation types, described by Bouchet et al. (2011). *Agathis-Calophyllum* Kauri-Tāmanu forest, is only found in the northern Cumberland Peninsula, above 600 m above sea level (a.s.l.), in the few areas where it was not logged in the 19th and early 20th centuries. Medium-stature forest is much more widespread across

the west coast of Santo. Many of the trees are tall and especially at lower elevations some deciduous species can be found such as *Pterocarpus indicus* (Fabaceae). The most characteristic element is *Castanospermum australe* (Fabaceae), one of the largest trees of this forest type. The subcanopy of medium-stature forest includes species such as *Dendrocnide latifolia* and *Pipterus argenteus* (Urticaceae). Where this forest type is disturbed, a number of secondary forest taxa become dominant including *Macaranga* spp. and *Rapanea* spp. (M. Prebble pers obs.) along with Arecaceae palms and *Pandanus* spp. At higher elevation (>500 m a.s.l.) the subcanopy changes to *Meryta neoebudica* (Araliaceae), *Myristica inutilis* (Myristicaceae) and *Ficus septica* (Moraceae). Finally, montane cloud forest, now found above 800 m a.s.l., is typically dominated by species belonging to several genera, including *Metrosideros* and *Syzygium* (Myrtaceae), *Weinmannia* and *Geissois* (Cunoniaceae), *Quintinia* (Quintiniaceae) and *Ascarina* (Chloranthaceae). Seasonal forest, scrub and grassland are characteristic of many of the coastal lowland areas in close proximity to villages. In exceptionally dry areas that are frequently burnt, these forests are dominated by *Acacia spirorbis* (Fabaceae) and *Kleinhovia hospita* (Malvaceae). These areas were heavily exploited in the mid-19th century for the sandalwood trade (Shineberg, 1967), with *Santalum* spp. now rare in Santo.

1.2 Archeological background and European contact

Lapita archeological sites are the most ancient sites attesting to human presence in the archipelago of Vanuatu (Bedford and Spriggs, 2018). Archeological findings suggest that Santo was initially settled approximately 3000 years BP, particularly in the vicinity of Big Bay and Port Olry (Figure 1), where Lapita pottery shards associated with early settlements have been found (Bedford and Spriggs, 2008; Bedford, unpublished data). From here, it has been hypotesized that people gradually spread across the small islands to the east and south of Santo (Galipaud, 2011). Malo, a small island to the south of Santo, provides evidence of initial settlement dating back around 2850 years BP (Galipaud, 2000). However, it has been suggested that these early settlements were abandoned by around 2000 years BP, possibly in response to changing environmental conditions (Galipaud, 2011). The occupation of the west coast of Santo may have been later than in Big Bay, Port Olry or Malo. Excavations near Cape Cumberland on the northwest coast produced dates of 1000 years BP, revealing evidence of irrigated agriculture remains (Galipaud, 2004; Figure 1). Another excavation at the Malsosoba shelter, in the northwest of Santo, revealed pottery shards dating back 1000 years BP and a pig's molar dating back 300 years BP (Galipaud and Walter, 1997; Galipaud, 2004; Tzerikiantz, 2006). The remoteness of west coast Santo has greatly limited archeological research, but it is highly likely that older settlement sites exist in the region. Oral traditions of settlement patterns in the region do point to substantial mobility throughout the coast and interior prior to European contact (e.g. Speiser, 1913).

Santo was the first island of the Vanuatu archipelago to be contacted by Europeans when Portuguese explorer Pedro Fernandes de Queirós arrived in Big Bay in 1606 CE, naming the islands "Australia del Espiritu Santo" (Deser et al., 2004; Figure 1). De Queirós and his crew settled in Big Bay for 40 days. This settlement represents one of the earliest European settlements in Remote Oceania (Moorehead, 1987; Berrocal and Sand, 2021; Sand, 2023). In his accounts, de Queirós reports a well-populated region, with cultivations and inhabitants engaged in pottery-making, however the accuracy of his reporting is questionable (Jolly, 2009). The contact with the local population was brief and conflictual and it is probable that diseases were introduced with a detrimental impact on local people (Marshall, 1937), as was experienced throughout Pacific Island societies (Moorehead, 1987; Kirch and Rallu, 2007).

2 Materials and methods

2.1 Study sites, field measurements and sampling

The coring campaign was conducted in July 2017 using a percussion corer (UWITEC, Mondsee, Austria) equipped with a 63 mm diameter PVC tube. Two sediment cores were retrieved from the center of two ponds (Richardson et al., 2022) located on the west coast of Santo (Figure 1): Nopovois, also known as Lac Soulematsi (15°29′49.14″S 166°44′8.30″E, 121 cm long), and Wunavae (15°

6′42.33″S 166°39′39.60″E, 83 cm long) following the toponymy assigned by local inhabitants in absence of official names. Cores were sectioned on-site at 1 cm intervals and stored in Whirl-Paks® at −20°C. Samples were then freeze-dried and macrofossils separated from the sediment matrix.

Nopovois is located 370 m a.s.l., has a perimeter of 500 m at the maximum height of water level, and a 59.4 ha catchment. The lake is mainly rain-fed with drainage probably to the north east occurring only during peak overflows in high rainfall episodes. Local residents indicated that the lake rose by a number of meters during Cyclone Pam in March 2015. A multiparameter depth sonde (IDS) was used to measure the maximum water depth during coring (2.6 m on July 25, 2017), and the surface temperature, which varied from 24.3°C in the morning to 26.7°C in the afternoon. Conductivity was stable at 96.7 µS/cm, while dissolved oxygen went from 5.39 mg/L to 8.61 mg/L and pH from 6.9 to 7.4, between the morning and the afternoon. Near bottom waters at 2.6 m water depth (w.d.) had a temperature of 23.5°C, conductivity of 108 µS/cm, dissolved oxygen between 0.01–0.02 mg/L, and a pH of 6.6 at both times of the day. Nopovois is located 300 m from a village which, at the time of coring, was composed of ca. 10 traditional houses. Coconut plantations, other tree crops, taro, and peanuts are the main crops cultivated in the catchment. Secondary forest dominates the uncultivated areas in the lake vicinity, with primary forest restricted to areas above 800 m a.s.l. in elevation and a further 4.5 km inland.

Wunavae is located 490 m a.s.l. and has a catchment of 4.95 ha and a perimeter of 300 m. The surrounding topography of the lake suggests that it may have been impounded by a now forest-covered landslip to the northwest. Similar landslides may have also impounded Lake Nopovois. The lake is mainly rain-fed, with no obvious outflow observable, although overflow probably occurs to the south during high rainfall episodes. The maximum lake depth at the time of coring (July 22, 2017) was 2.8 m. The near surface water (0.2 m w.d.) had a temperature of 22.7°C at midday (red dot in Figure 4), conductivity of 233 µS/cm, dissolved oxygen of 0.1 mg/L, and a pH of 6.3. Temperature decreased to 21°C near the bottom (2.5 m w.d.), while conductivity increased to 334 µS/cm, dissolved oxygen decreased to 0.02 mg/L, and pH increased to 6.7. Wunavae was almost entirely covered with aquatic plants, and surrounded by a high canopy semi-deciduous seasonal forest reflecting the typical secondary forest vegetation of this part of the island (Bouchet et al., 2011). The direct surroundings of lake Wunavae were uninhabited, the closest village being located on the coast around 2.8 km to the west. Relatively undisturbed primary forest, including Agathis, Podocarpaceae and *Campnospermum* remnants lie above 800 m a.s.l., around 4.5 km to the east of the lake.

2.2 Chronology

Eighty-two macrofossils were selected for radiocarbon dating from Nopovois and seventy from Wunawae (Supplementary Figure S1). After an Acid-Base-Acid chemical treatment to remove carbonates and humic acids, samples were transferred to pre-cleaned Al-boats and weighed. Radiocarbon measurements were performed using gas ion source accelerator mass spectrometry (AMS) on the

compact Mini Carbon Dating System (MICADAS) at the Laboratory of Ion Beam Physics, ETH Zürich, Switzerland. To account for constant contamination, two sets of standards, fossil (PhA, n = 42) and modern (Oxa II, n = 39), were added to each sequence. Modern 1515 wood and radiocarbon-depleted Kauri wood were added as reference material. Processing standards and reference material were added at different C masses.

The age of sediment deposition was modeled using the r package rbacon version 2.5.8 (Blaauw and Christen, 2011). Radiocarbon dates were calibrated with the Southern hemisphere calibration curve SHCal20 (Hogg et al., 2020). Samples with $F^{14}C$ >1 and above 60 cm were calibrated using the online calibration software CALIBomb (Reimer and Reimer, 2023) and the SH1-2 calibration curve (Hua et al., 2022).

The upper 40 cm of both cores reveal post bomb dates and are investigated in detail in another study focusing on the last century (Camperio et al., 2024). The age model from 42 to 121 cm in the Wunavae sediment record is based on 35 radiocarbon-dated macrofossils, while 38 radiocarbon-dated macrofossils constrain the age model from 42 to 83.5 cm in the Nopovois sediment record. Bayesian age depth models provide a bottom age of 943–1042 CE for Wunavae and 813–1041 CE for Nopovois. The average sedimentation rate for the lower core section in Nopovois is 0.04 cm/yr while it reaches 0.08 cm/years in Wunavae. The age model uncertainty for both Wunavae and Nopovois in these lower core sections averages ~75 years. Hence comparisons between these West Santo sites and other sites across the Pacific are limited to centennial scale. The frequent plateaus in the calibration curve between 1600 and 1800 CE coupled with high accumulation rates in the upper part of the cores (after 1960 CE) increase the uncertainty in this time window for lake Nopovois. The low sedimentation rate could potentially indicate a hiatus between 1600 and 1900 CE.

2.3 Bulk geochemistry

The number of samples reported in this section refers to the period of interest, namely section 42–121 cm for Lake Wunavae and section 42–83.5 cm for Lake Nopovois. Bulk geochemical analyses were carried out in the Sedimentology laboratories at Eawag, Dübendorf. Downcore total carbon (TC) and total nitrogen (TN) content of 40 samples for Wunavae and 25 for Nopovois were measured with an EURO Elemental Analyser (EA) 3000 (HEKAtech GmbH, Wegberg, Germany). Total inorganic carbon (TIC) was measured with a titration Coulometer (CM5015, UIC Inc., Joliet, United States). Total organic carbon (TOC) was calculated using the equation TOC = TC - TIC. The atomic ratio between TOC and TN was calculated in the section of interest. Forty samples from Wunavae and 25 from Nopovois were measured for biogenic silica (BiSi) concentrations following the method by Ohlendorf and Sturm (2008). Standards for aluminum (Fluka analytical, Lot Nr. 1404169), silicon (J.T. Baker, Lot Nr. N081093), and sodium (J.T. Baker, Lot Nr. N082168) were used for BiSi quantification. Grain size measurements were performed at 2 cm resolution for both cores. Sediment samples were dispersed in $NaPO_4$ and placed overnight in an overhead shaker prior to being measured with a Beckman Coulter LS 13 320 (laser diffraction particle analyzer).

2.4 Biomarkers

Lipid extraction, purification and quantification were performed in the Sedimentology laboratories at Eawag, Dübendorf. All glassware used with biomarker samples was ashed at 450°C for 5 h. A known amount of recovery standard composed of 5a-androstane, 1-nonadecanol, heneicosanoic acid and 3-eicosanone was added to the freeze-dried, homogenized sediment. Lipids were extracted from 40 samples of the Wunavae core (section 41–121 cm) and 20 samples of the Nopovois core (section 41–83.5) evenly distributed along the core length. A mixture of Dichloromethane:Methanol (DCM/MeOH, 9:1, v/v) was used for the extraction with a Dionex ASE 350 (Thermo Scientific). If available, a maximum of 3 g of dry sediment was processed, otherwise, smaller quantities were used. The total lipid extracts were dried under a gentle nitrogen stream before saponification with 3 mL of 1 N KOH in MeOH and 2 mL of solvent-extracted ultrapure water at 70°C for 3–16 h. Lipids were liquid-liquid extracted from the aqueous phase using 2 mL hexane three times, generating the neutral fraction. The remaining aqueous phase was acidified to pH <2 with 4 N HCl, and the protonated fatty acids were recovered using liquid-liquid extraction with 4 mL hexane three to four times. Fatty acids were methylated by adding 7 mL of MeOH:HCl (95:5) solution to each fatty acid sample and heating to 70°C for 12 h. After cooling, 7 mL of solvent-extracted ultrapure water was added to the samples and fatty acid methyl esters (FAMEs) were recovered by liquid-liquid extraction using 4 mL hexane (rinse done three to four times). For samples in which FAMEs were abundant enough (Wunavae n = 27, Nopovois n = 21) for gas chromatography-isotope ratio mass spectrometry (GC-IRMS), $AgNO_3$-Silica Gel (~10 wt% loading) was used to purify FAMEs for hydrogen isotope ratio (δ^2H) measurements.

ISOLUTE® SI 500 mg/6 mL Silica gel columns (Biotage, Uppsala, Sweden) were used to separate the neutral fraction into four subsequent fractions: 1) hydrocarbons including *n*-alkanes (4 mL of hexane), 2) ketones and aldehydes (4 mL of hexane/DCM, 2:1, v/v), 3) sterols and other alcohols (4 mL of DCM/MeOH, 19:1, v/v), 4) more polar compounds (4 mL of MeOH). In the third fraction, compounds with hydroxyl groups were converted into trimethylsilyl derivatives prior to analysis by adding 25 μL each of N,O-bis-(trimethylsilyl) trifluoroacetamide (BSTFA) and pyridine and heating to 60°C for 1 hour.

Compounds were identified and quantified by gas chromatography–mass spectrometry (GC–MS). The GC–MS analyses were performed on an Agilent 7890B gas chromatograph with an Agilent HP-5MS column (30 m × 0.25 mm × 0.25 mm film thickness) coupled with an Agilent 5977B mass spectrometer (MS) and a flame ionization detector (FID) (Agilent Technologies, Santa Clara, United States). Ketones and the derivatized sterols were analyzed using a Selected Ion Monitoring method targeting *m/z* 215 (quantified), 355, 370 for coprostanol and epicoprostanol and *m/z* 71, 239, 255 (quantified) for palmitone. External standards containing the targeted compounds were analyzed for identification and quantification using an external calibration curve (abcr GmbH, 16-Hentriacontanone Lot 1398514 for palmitone, Sigma-Aldrich CAS 360-68-9 Lot 0000188007 for coprostanol, and Sigma-Aldrich CAS 516-92-7 Lot 127M4099V for epicoprostanol). We consider fecal sterols as the sum of coprostanol and epicoprostanol. Fatty acids and alkanes were run in Total Ion Scan mode and

quantified with the internal standards (5α-androstane for alkanes and heneicosanoic acid for the fatty acids) and normalized to gram TOC. Agilent Mass Hunter was used for identification and peak integration.

Based on the *n*-alkane quantities (C_X refers to the total or relative compound content in a sample in all relevant equations), the Paq ratio (Equation 1) was used to identify potential contributions from aquatic plants, calculated according to Ficken et al. (2000):

$$Paq = \frac{C_{23} + C_{25}}{C_{23} + C_{25} + C_{29} + C_{31}} \qquad (1)$$

This ratio is based on the assumption that C_{23} and C_{25} are mainly produced by macrophytes. Modern plants give values that can be used as proxy for emergent aquatic plants (0.1–0.4), submerged aquatic plants (>0.4), and terrestrial plants (<0.1), keeping in mind that sediment samples can reflect different sources (Ficken et al., 2000). Based on fatty acid quantities, the terrigenous to aquatic ratio (TAR, Equation 2) is calculated following (Tenzer et al., 1999; Fang et al., 2014):

$$TAR = \frac{C_{24} + C_{26} + C_{28}}{C_{12} + C_{14} + C_{16}} \qquad (2)$$

The TAR is interpreted as relative contributions of fatty acids of either terrigenous (TAR >4) or aquatic (<2) origin (Tenzer et al., 1999; Fang et al., 2014). *n*-Alkane average chain lengths (ACL_{27-33}, Equation 3) were calculated as (Poynter and Eglinton, 1990):

$$ACL_{27-33} = \frac{27 \cdot C_{27} + 29 \cdot C_{29} + 31 \cdot C_{31} + 33 \cdot C_{33}}{C_{27} + C_{29} + C_{31} + C_{33}} \qquad (3)$$

Fatty acid ACL_{22-30} (Equation 4) was calculated following Eglinton and Hamilton (1967):

$$ACL_{22-30} = \frac{22 \cdot C_{22} + 24 \cdot C_{24} + 26 \cdot C_{26} + 28 \cdot C_{28} + 30 \cdot C_{30}}{C_{22} + C_{24} + C_{26} + C_{28} + C_{30}} \qquad (4)$$

Underivatized aliquots (10%) of fractions 3 and 4 were recombined for brGDGTs analysis. Samples were filtered using a 0.45 μm PTFE filter prior to analysis using high-performance liquid chromatography–atmospheric pressure chemical ionization–mass spectrometry (HPLC-APCI–MS), as described by Hopmans et al. (2016), with a modified column temperature (40°C). Detection was achieved in selected ion monitoring mode for *m/z* 1,050, 1,048, 1,046, 1,036, 1,034, 1,032, 1,022, 1,020 and 1,018 for brGDGTs. Agilent Chem Station software was used to integrate peak areas. Branched GDGTs analyses were conducted at the Biogeoscience laboratory at ETH Zurich. Mean annual temperature reconstruction based on brGDGTs was obtained following the Zhao et al. (2023) tropical calibration regression, since a ternary diagram revealed that the dataset at the basis of the Zhao et al. (2023) calibration matches the distributions of the downcore data presented in this manuscript best (Supplementary Figure S2). We applied the following Equation 5 (Zhao et al., 2023):

$$\text{Mean annual air temperature (MAAT)}$$
$$= -1.78 \ (\pm 0.42) + 31.01 \ (\pm 0.60) \times MBT'5ME \qquad (5)$$

The $\delta^2 H_{LW}$ analyses were performed in the Biogeochemistry Laboratory at Eawag's Center for Ecology, Evolution, and Biogeochemistry in Kastanienbaum. The samples were analyzed on a Trace GC Ultra gas chromatograph (GC) coupled to a Thermo Delta V Plus isotope ratio mass spectrometer (IRMS) *via* a GC Isolink operated in pyrolysis mode and ConFlo IV interface (Thermo Fisher Scientific, Bremen, Germany). The measured values were normalized to the VSMOW/SLAP scale using hydrogen isotope standards purchased from Arndt Schimmelmann at Indiana University (mix C4, *n*-C_{28}-alkane #1, *n*-C_{32}-alkane #1), which were analyzed at the beginning and end of each sequence, as well as after every ~10 sample injections. Measurement accuracy and precision were assessed from a quality control standard, a hydrocarbon fraction from oak leaves that were originally collected in Berkeley, California, which has a long term $\delta^2 H$ value of −138‰ ± 5‰ (n = 343). During the analysis window, the $\delta^2 H$ value of this standard averaged −135‰ ± 3‰ (n = 19). The $\delta^2 H$ value of hydrogen added during methylation was determined by methylating phthalic acid of known isotopic composition (Arndt Schimmelmann, Indiana University), and fatty acid $\delta^2 H$ values were corrected using isotopic mass balance.

2.5 Pollen and charcoal

Palynomorph analyses (including pollen and spores) were conducted at a 5 cm resolution downcore. Each 1 cm³ sample was processed using standard procedures (10% HCl, hot 10% KOH, and acetolysis; Moore et al., 1991). Samples were spiked with exotic *Lycopodium clavatum* L. tablets to allow the palynomorph and charcoal concentrations to be calculated. Counts continued until reaching at least 100 terrestrial palynomorphs. Palynomorphs were identified by comparison with the reference collection held at the Australian National University and with the Australasian Pollen and Spore Atlas (https://apsa.anu.edu.au/). The vegetation types (primary, secondary, dryland herbs, *etc.*) were determined from regional and local syntheses of Pacific Island plant ecology (Mueller-Dombois and Fosberg, 1998; Bouchet et al., 2011). The charcoal particle counts are based on particles <125 microns, as they were counted on slides prepared for pollen.

3 Results

Most proxies followed similar downcore trends in Wunavae and Nopovois (Figure 2; Supplementary Figure S3). The higher sampling resolution of Lake Wunavae allows for a more detailed reconstruction of changes, which appear to be closely reflected in the Lake Nopovois core. Unless specified, the results described and discussed below thus refer to Lake Wunavae. The results provided hereafter are based on median calibrated ages. The age ranges are available in Camperio et al. (2024). Interpretation guidelines for each proxy are provided in Table 1.

3.1 1000−1300 CE

Charcoal particles were present in the basal samples of both cores suggesting that sedimentary accommodation spaces were created in part through human modification of the landscape at around 1000 CE. Charcoal particles increased to a maximum
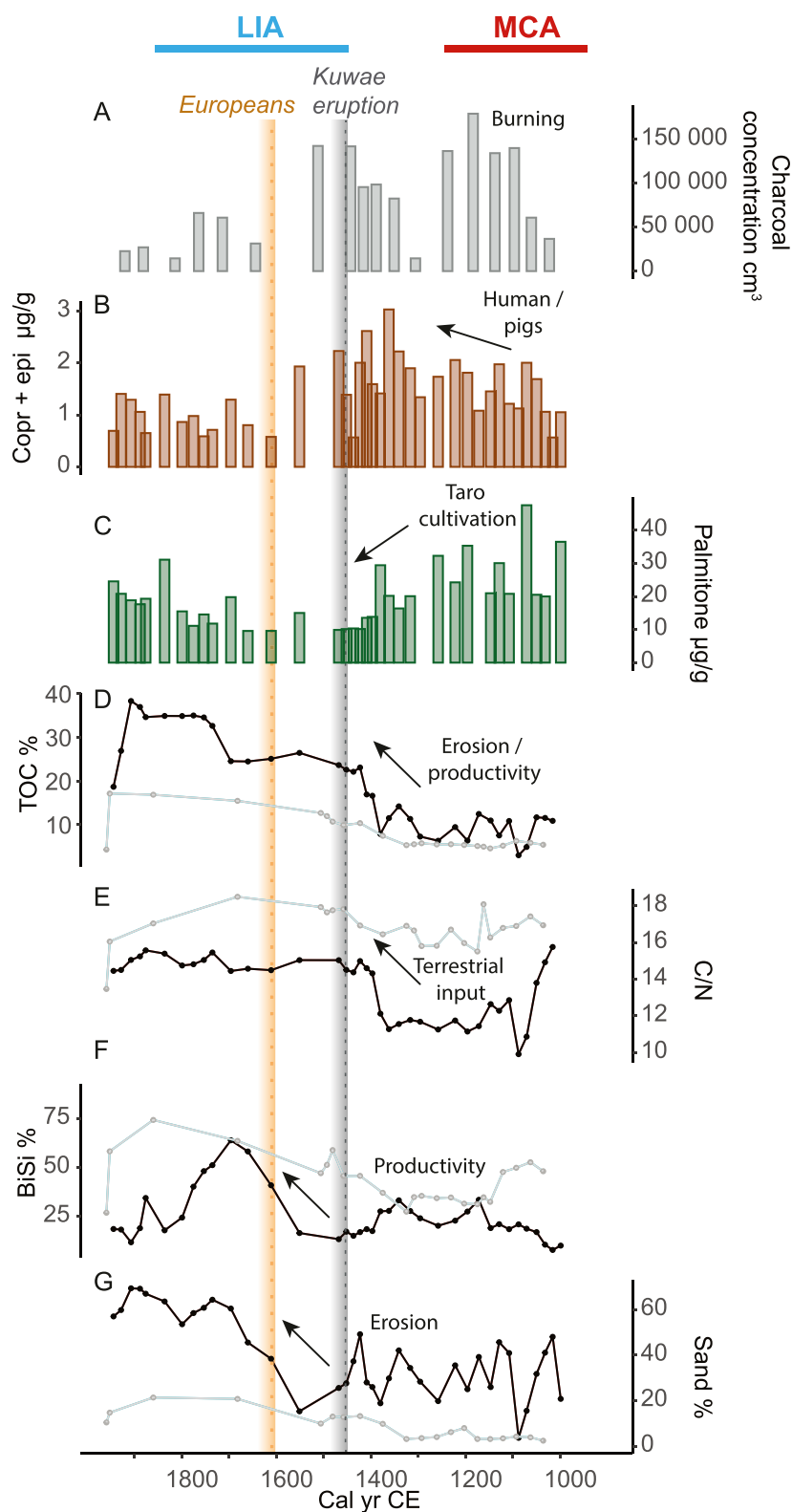
FIGURE 2
Proxies for human presence and activities, and environmental changes from Lake Wunavae and Lake Nopovois, west Santo. **(A)** Charcoal concentration (grains/cm³), **(B)** fecal markers (coprostanol + epicoprostanol, brown) and **(C)** palmitone (green) concentrations (µg/g TOC) from Wunavae. **(D)** TOC (%), **(E)** C/N, **(F)** BiSi (%) and **(G)** sand (%) from Wunavae (black lines) and Nopovois (light gray). The grey dotted line shows the timing of the Kuwae eruption (1452 CE). The yellow dotted line marks the European arrival in 1606 CE.

TABLE 1 Interpretation of proxies in west Santo. More detailed explanation can be found in the Supplementary Material.

Proxy	Interpretation	References
Human Traces		
Microcharcoal concentration	Burning	Kershaw et al. (1997)
Fecal molecules	Omnivores feces (presence of humans, pigs)	Bethell et al. (1994); Bull et al. (2003)
Palmitone Crop pollen	Taro cultivation - horticulture Horticulture	Krentscher et al. (2019)
Terrestrial and Aquatic Ecosystem Changes		
Total Organic Carbon (TOC%)	Changes in erosion and productivity	Meyers and Teranes (2001)
C/N values	Submerged/emerged/terrestrial vegetation	Meyers (1994); Xia et al. (2014); Gong et al. (2018)
BiSi	Diatoms – lake productivity and water level	Conley and Schelske (2001)
Sand	Erosion (+)	Håkanson and Jansson (1983)
Clay	Tephra layers (++)	Lowe and Nelson (1983); Cashman and Rust (2016)
Pollen	Vegetation	Mueller-Dombois and Fosberg (1998)
Paq	Aquatic vegetation	Ficken et al. (2000)
TAR	Relative sources of short and long chain fatty acids	Tenzer et al. (1999); Fang et al. (2014)
ACL	Terrestrial vegetation – grass (+)	Eglinton and Hamilton (1967); Poynter and Eglinton (1990)
Climatic Proxies		
δ^2H of longer-chain fatty acids	Precipitation isotopes	Ladd et al. (2021); see also section 4.1
MBT'5 ME	temperature based on brGDGT distribution	De Jonge et al. (2014)
MAAT brGDGTs	Mean Annual Air Temperatures	Zhao et al. (2023)

of 180,000 grains/cm^3 at around 1200 CE (Figure 2A). Fecal sterols, despite some minor fluctuations, were stable at 1.5 ± 0.1 µg/g (Figure 2B; Supplementary Figure S3). Palmitone was most abundant at the bottom of the core in Wunavae with the highest peak around 1100 CE with 48 µg/g, while it maintained sustained concentration (29 ± 3 µg/g) in Nopovois (Figure 2C). Minor fluctuations between 8.2% and 9.8% characterized TOC content of Wunavae in this period (Figure 2D). In Nopovois, TOC was stable around 5 ± 0.8%. This low TOC was consistent with a peak in clay (Supplementary Figure S4) which indicated the presence of a microtephra also observed during pollen analysis in both cores. C/N decreased from a maximum value of 16 at the bottom of the Wunavae core to a minimum of 9 around 1100 CE (Figure 2E). In Nopovois, C/N maintained stable values between 11.6 and 12.4. Biogenic silica was stable in Wunavae during this interval, with an average of 20 ± 2% and only one small peak around 1100 CE possibly linked to the tephra layer (Figure 2F). The sand content fluctuated greatly between 20% and 45% in Wunavae, while it only fluctuated between 3% and 7% in Nopovois (Figure 2G). In Wunavae, the landscape was dominated by secondary forest (Figure 3), with notable abundance of ferns and dryland herbs. Conversely, in

Nopovois, grassland prevailed as the primary vegetation type, followed by secondary forest, wetland herbs, and ferns. δ^2H values of long-chain fatty acids (n-C$_{26}$, -C$_{28}$ and -C$_{30}$) show large fluctuations and variable offsets from each other. The Paq ratio ranged between 0 and 0.2 (Figure 4B), ACL$_{27-33}$ showed high variability, between 28 and 30 (Figure 4C). The TAR ratio was stable around 4 (Figure 4D) while ACL$_{22-30}$ started decreasing slightly from 27 around 1000 CE to 26 around 1300 CE (Figure 4E). brGDGT-based mean annual air temperature (MAAT) fluctuated with a decreasing trend from 24°C around 1000 CE to a minimum of 21°C around 1200 CE (Figure 4F).

3.2 1300−1500 CE

During this time interval, changes were observed across several proxy indicators. In Wunavae, charcoal concentrations reached 140,000 grains/cm^3 (Figure 2A), while fecal sterols reached their highest concentration of 3 µg/g in 1362 CE (Figure 2B). In contrast, the concentration of palmitone experienced a sharp decline (Figure 2C), maintaining a minimum concentration for this period at 10 ± 0.1 ug/g from ca. 1400 to 1450 CE. This sharp palmitone
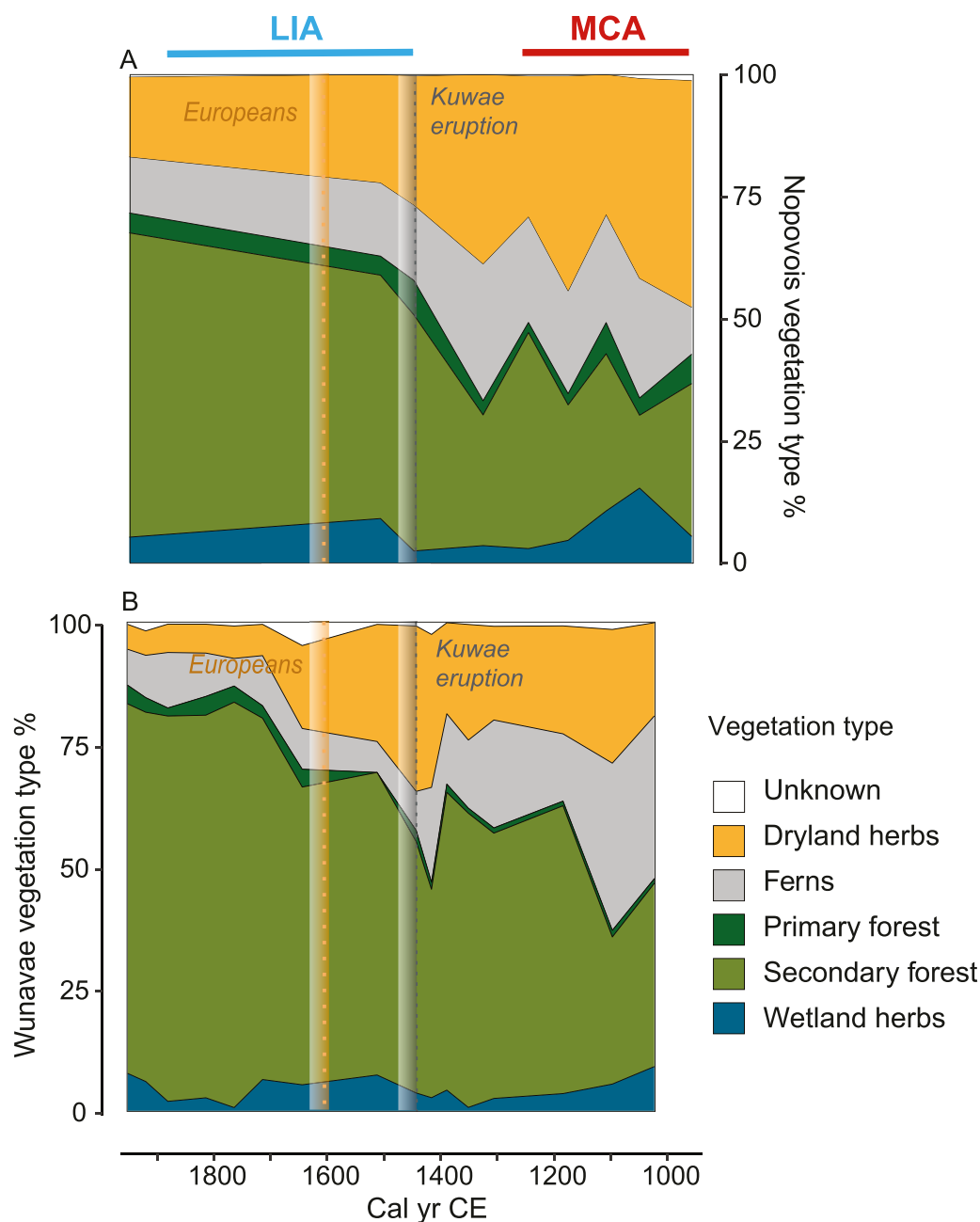
FIGURE 3
Regional vegetation changes in west Santo. Vegetation type (%) for Nopovois **(A)** and Wunavae **(B)**, with unknown pollen in white, wetland herbs in blue, secondary forest in light green, primary forest in dark green, ferns in grey, and dryland herbs in orange. Following Figure 2, the grey dotted line shows the timing of the Kuwae eruption (1452 CE). The yellow dotted line marks the European arrival in 1606 CE.

decline was not consistently observed in Nopovois. Both TOC% and the C/N ratio showed a step-like increase in Wunavae around 1400 CE, reaching a maximum TOC of 23% around 1420 CE (Figures 2D,E). Subsequently, a sudden decrease was recorded in charcoal, fecal sterols, and palmitone around 1500 CE in Wunavae. Meanwhile BiSi% remained relatively stable (Figure 2F), around 22 ± 2%. Sand content exhibited substantial variability, with alternating peaks between 50% and lows of 20% (Figure 2G). In Nopovois, TOC%, C/N, BiSi%, and sand% all showed a slight increase.

In Wunavae, dryland herbs, dominated by grass, reached their maximum around 1450 CE (Figure 3). The $n\text{-}C_{28}$ δ^2H values reached their highest value of $-112 ± 2‰$ around 1400 CE (Figure 4). Both Paq and TAR recorded significantly more elevated values between 1400 and 1500 CE, with Paq reaching its maximum of 0.8 and TAR its maximum value of 12 in 1400 CE. Meanwhile, $ACL_{27\text{-}33}$ recorded lower values (28.5) in the interval 1300–1400 CE, followed by a clear shift to higher values in the interval 1400–1500 CE (30), while $ACL_{22\text{-}30}$ showed the opposite pattern with higher values
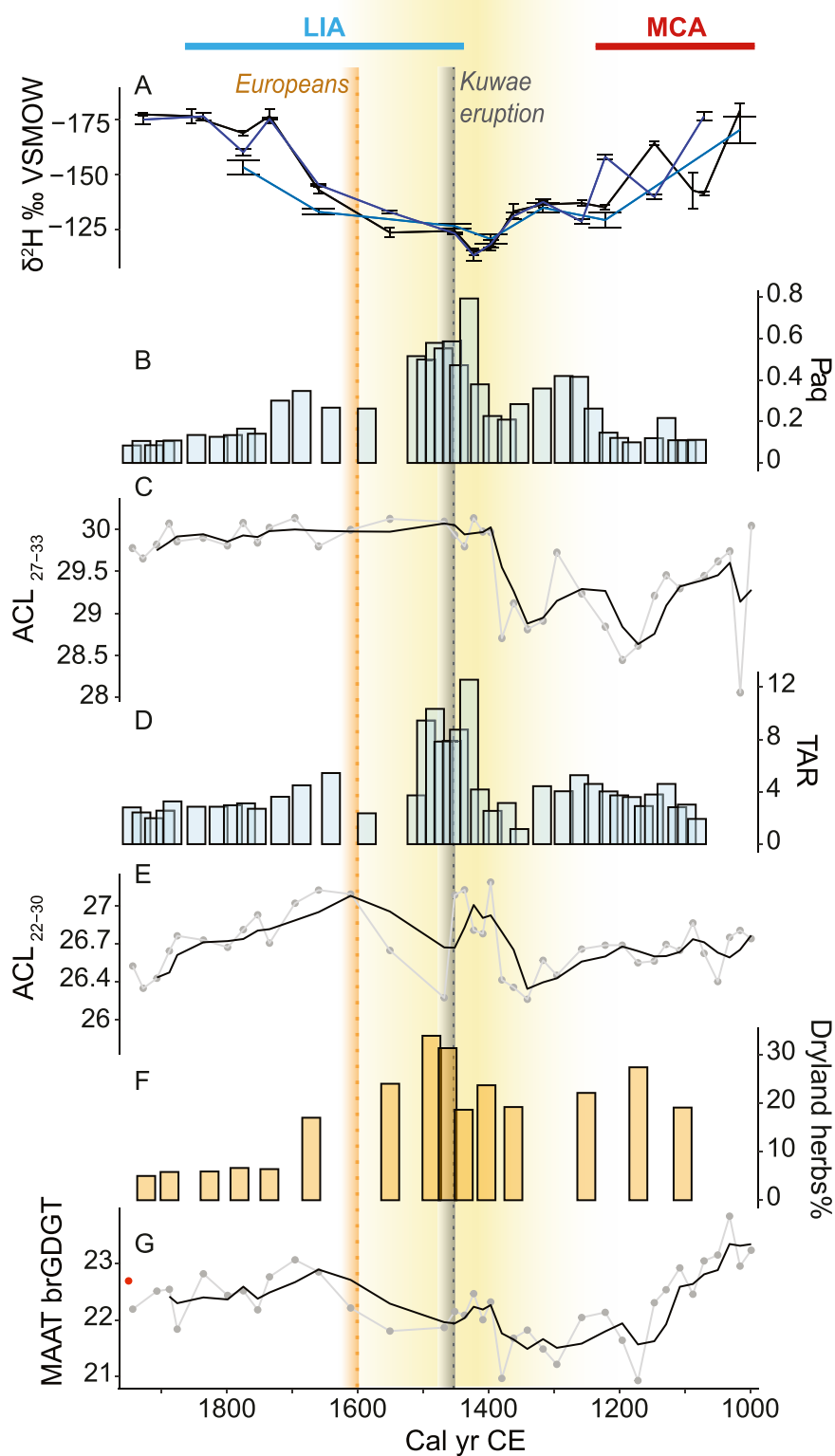
FIGURE 4
Last millennium climatic signal from Wunavae, west Santo. **(A)** δ²H values of *n*-C$_{26}$ (teal), *n*-C$_{28}$ (black), *n*-C$_{30}$ (blue), **(B)** *n*-alkane Paq, **(C)** *n*-alkane ACL$_{27-33}$, **(D)** TAR, **(E)** fatty acids ACL$_{22-30}$ **(F)** pollen from dryland herbs, **(G)** MAAT brGDGT using the calibration by Zhao et al. (2023). Black lines represent the 3-point running mean. Yellow shading indicates the drier period. The Medieval Climate Anomaly (MCA) and Little Ice Age (LIA) periods are respectively indicated with a red and blue line. As in Figure 2, the grey dotted line shows the timing of the Kuwae eruption (1452 CE). The yellow dotted line marks the European arrival in 1606 CE. The red dot indicates the lake surface temperature in 2017.

from 1300 to 1400 CE, and lower values from 1400 to 1500 CE. Finally, MAAT from brGDGTs maintained minimum values around 21°C from 1200 to 1400 CE, followed by a slight increase to 22°C around 1500 CE.

3.3 1500−1800 CE

During this timeframe, charcoal concentrations (50,000 ± 15,000 cm^3), fecal markers (1 ± 0.1 μg/g), and palmitone concentrations (17 ± 2 μg/g) all reached their lowest values (Figures 2A,B–C). However, there was a notable step increase in TOC% around the year 1700 CE (Figure 2D), while C/N values remained predominantly stable throughout this period (Figure 2E). BiSi% experienced a long and significant peak between 1550 and 1800 CE, reaching its highest value by 1700 CE (Figure 2F). The sand content steadily increased, with a peak of 64% by 1700 CE (Figure 2G).

Dryland herbs declined in both cores, with a sharp decrease in Poaceae noted in Wunavae after 1700 CE (Supplementary Figure S5). Secondary forest vegetation became prevalent in the landscape during this period, accompanied by an increase in *Macaranga* observed in both ponds. In Wunavae, there was also notable growth of *Phyllanthus* and *Pandanus* (Supplementary Figure S5). Additionally, *Botryococcus* algal colonies indicative of stable water bodies, made their initial appearance in both lakes at this time (Supplementary Figures S6–S9).

The n-C_{28} δ^2H values exhibited a continuous decline, reaching −179 ± 3‰ around 1750 CE (Figure 4). Both Paq and TAR values declined relatively steadily following their peak. While ACL_{27-33} remained constant throughout this interval (30), reaching its maximum level in the youngest layers, ACL_{22-30} first increased until 1600–1700 CE and then decreased steadily. MAAT brGDGT showed an increase, with a peak in 1700 CE, following a similar trend as BiSi.

4 Discussion

We produced records of climate and human activities from sediment cores from two ponds on the west coast of Espiritu Santo, Vanuatu. The multi-proxy records revealed three different hydroclimatic phases over the last millennium and two contrasting intervals of human-related activities. Charcoal, palmitone and fecal markers were present from the beginning of the record at 1000 years BP (1000 CE), and decreased significantly by 1400 CE (Figures 2A–C), when TOC% and the C/N ratio revealed a large step-like increase (Figures 2D,E) and the pollen recorded an increase in secondary forest (Figure 3). In the following discussion we place these results in the broader climatic context, and consider the possible effects that the hydroclimatic changes had on the inhabitants.

4.1 Interpretation of fatty acid δ^2H values in West Santo pond sediments

Globally, long-chain fatty acid δ^2H values are strongly correlated with δ^2H values of mean annual precipitation, a relationship that forms the basis of using sedimentary plant waxes to reconstruct past precipitation δ^2H values (Sachse et al., 2012; McFarlin et al., 2019; Ladd et al., 2021). Long-chain fatty acid δ^2H values from core top sediments from the tropical Pacific fit this global pattern, but there is considerable scatter around the linear regression between δ^2H_{FA} and δ^2H_P values, both in tropical Pacific lakes and elsewhere (Ladd et al., 2021). Part of this scatter may be due to variable inputs from different plant sources, which can have large differences in apparent fractionation between source water and plant waxes (Gao et al., 2014; Baan et al., 2023; 2025). As such, before interpreting changes in δ^2H_{FA} values solely in terms of changes in δ^2H_P, potential effects from changing vegetation sources need to be considered, particularly in the context of small lakes with limited catchments, which are more susceptible to shifting vegetation sources (Hirave et al., 2023).

In the absence of major changes in the sources of fatty acids to sediments, overall distributions of fatty acid homologues and the relative offsets between their δ^2H values are expected to remain constant. In the case of fatty acids from Wunavae sediments, some shifts in fatty acid sources seem to have occurred over the past millennium. In particular, maximum δ^2H_{FA} values around ~1450 CE coincide with marked changes in fatty acid distributions, indicated by high TAR, high ACL and high Paq values (Figure 4). At the same time, n-alkane distributions change, with the highest Paq values of the record occurring during the same interval as the highest δ^2H_{FA} values (Figure 4). Likewise, offsets among long-chain fatty acid δ^2H values fluctuate throughout the record, suggesting variable sources of these compounds. Taken together, these results suggest that the ~70‰ decline in δ^2H_{C28} values from ~1750 to 1900 CE is unlikely to be driven by a correspondingly large decline in δ^2H_P values.

Although the magnitude of change for δ^2H_P values is difficult to determine given the potential effects of different fatty acid sources, relative ^{2}H-enrichment of all long-chain homologues in both Wunavae and Nopovois sediments during the interval from ~1250 to ~1750 CE suggest that δ^2H_P values were relatively ^{2}H-enriched during this time. As these ponds are located in a significant rain shadow, local δ^2H_P values are impacted by orographic effects (Ladd et al., 2021), similar to other mountainous tropical settings (Scholl et al., 1996; Sánchez-Murillo et al., 2020). These orographic effects make it challenging to interpret changes in δ^2H_P values solely in terms of the amount effect (i.e., wetter sites have lower δ^2H_P values), because this is only observed for coastal/sea level tropical sites (Dansgaard, 1964; Risi et al., 2008; Conroy et al., 2013). Nevertheless, model results suggest that regional δ^2H values of water vapor and precipitation around Vanuatu increase with weaker Walker circulation, such as during El Niño events (Prohaska et al., 2023), when the overall amount of precipitation in the archipelago also decreases.

The ^{2}H-enrichment of fatty acids from ~1250 to ~1750 CE coincides with a relatively high abundance of dryland herb pollen, as well as with changes in the lipid distributions that suggest greater contributions of n-alkanes and fatty acids from aquatic macrophytes. Increased relative abundance of material from aquatic plants could be caused by drying conditions, with shallower water leading to an expanded littoral zone and relatively less leaf biomass production by water-stressed terrestrial plants. Given

the challenges in interpreting $\delta^2 H_{FA}$ values through periods of vegetation change, we consider the pollen and plant wax distribution data to be stronger indicators of aridity in this setting. However, since increased aridity associated with El Niño events increases $\delta^2 H_P$ values around west Santo (Prohaska et al., 2023), and since $\delta^2 H_{FA}$ values are strongly correlated with $\delta^2 H_P$ values across large ranges of vegetation types, we suggest that the high $\delta^2 H_{FA}$ values from ~1250 to ~1750 CE in the Wunavae core were at least partly caused by higher $\delta^2 H_P$ values associated with weaker Walker circulation. As the vegetation sources likely changed during this time period, we consider it unlikely that the entire increase in $\delta^2 H_{FA}$ values was due to reduced precipitation. It is more likely that drought-induced changes in the sources of fatty acids to the pond's sediments were responsible for an unconstrained portion of the increase in $\delta^2 H_{FA}$ values.

4.2 Warmer and wetter conditions 1000 years BP favored the establishment of inland settlements and taro gardens in west Santo

Within the last millennium, linguistic variations became more marked in Vanuatu (Tryon, 1996) and pottery decorations diversified (Spriggs, 1997a; Bedford and Spriggs, 2018). On larger islands elsewhere in the tropical Pacific during the period, interior settlement became common. On Upolu, Sāmoa, for example, Cochrane et al. (2024) show a marked increase in inland horticultural features including stone walls and drainage ditches dated to within the last 800 years. They suggest that the newly developed areas of production in turn promoted territorial behaviour.

On west Santo, archeological records are still limited due to a lack of research, more than the lack of archeology, and only record the last 1000 years of occupation. The presence of charcoal at the bottom of both cores and most importantly the very similar age of their oldest layer suggests that these lakes may be engineered reservoirs. This is further confirmed by the bottom age of a third pond in the area, Lake Vesalea (Figure 1B), which was radiocarbon dated to 940 ± 78 cal years BP and has charcoal at the bottom (Krentscher et al., 2019). It is important to note that local informants suggest that Wunavae is not frequently visited today, however, the banks of Vesalea and Nopovois are currently cultivated for taro and other crops. The importance of these water sources is acknowledged, but whether their ancestors modified these ponds for the purposes of water storage was not determined.

As observed in other islands in the Pacific, settlement required land modifications, in particular forest clearance that increased the water yield and supplied sediment to impede drainage (Hope et al., 1999). Similar water management strategies have also been observed in the Maya Lowlands, where the ancient Maya used aguadas (either natural or human-made ponds) to collect rainwater, some of them having a plaster lining (Ferrand et al., 2012). The simultaneous initiation of pond development and possible engineering of these water reservoirs 1000 years BP likely helped facilitate inland expansion. Archeological evidence for taro gardens dating to 1000 years BP has been found in the northwest of Santo (Galipaud, 2004). Taro is a crop that prefers wet conditions, for which

Pacific Islanders developed specific cultivation techniques including terraced cultivation systems. Extensive taro irrigated systems are still present in the area today (Spriggs et al., 2012), some within close proximity (<2 km) from Vesalea, Wunavae and Nopovois. These engineered terraced pond field systems, similar to the lo'i terraced cultivations of the Hawaiian Islands, are highly adaptable, depending on hydrological conditions. The earlier development of other engineered hydrological features, such as water reservoirs, appears fitting in light of the extent and importance of terraced cultivation systems to the people of west Santo and in other large islands in the Western Pacific (e.g. West New Georgia, Solomon Islands, Bayliss-Smith et al., 2019).

Following this period of inland settlement and expansion of cultivation systems, there are, as yet, limited archeological findings indicating human activities in west Santo, with the exception of a site in northwest Santo that is dated to 1700 CE (Wirrmann et al., 2011), leaving a gap of 700 years without any indication of human presence or activities. In contrast to the patchy archeological record, the sedimentary archives we retrieved from Lake Wunavae and Lake Nopovois attest to the continuous presence of people in the region from 1000 to approximately 1500 CE, with activities like burning (charcoal) and planting (palmitone and crop pollen) (Figure 2). These findings would be in line with the demographic increase observed along with the expansion of agriculture starting 1000 years BP on the island of Efate, located further south in Vanuatu (Combettes et al., 2015; Bedford et al., 2018). The brGDGT-reconstructed temperatures suggest warmer conditions during the interval 1000–1200 CE (Figure 4; Supplementary Figure S9), while the relatively low n-C_{28} $\delta^2 H$ values are consistent with wetter conditions. Interpretation of the fatty acid $\delta^2 H$ values during this interval is the least robust of the record, as high contributions of fern pollen are associated with abnormal sedimentary fatty acid $\delta^2 H$ values in this region (Ladd et al., 2021), and because the large changes in relative offsets among $\delta^2 H$ values of different fatty acid homologues are indicative of shifting sources of fatty acids (Figure 4A). However, warm and wet conditions would have provided the ideal setting for the expansion of horticulture, and are consistent with evidence for taro cultivation during this interval.

4.3 Melanesian resilience to prolonged drought

Following the period of inland horticultural expansion, we observed a decline in palmitone starting around 1300 CE (Figure 2C). This interval was marked by a shift towards drier conditions, indicated by an increase in dryland herbs in Lake Wunavae starting at 1100 CE (Figure 3B) and an increase in $\delta^2 H_{FA}$ values. The orographic effect of the Cumberland Chain exacerbates the dryness in west Santo, where reservoirs might have dried out leading to a direct impact on both human populations and ecosystems. Droughts can lead to the depletion of freshwater resources, land degradation, and increased sedimentation in water bodies. Indeed, the TOC, C/N, TAR and Paq indicate an ecosystem shift around 1400 CE, led by a decrease in water level (Figures 2, 4). The lower water levels expanded the littoral zone, likely promoting the growth of macrophytes and resulting in high Paq values

(Figure 4B). These macrophytes may have outcompeted microalgae in the lake, which would account for the reduced TAR values we see during this interval (Figure 4D). Contrary to the usual interpretation of the TAR, in this context it indicates a disproportionate contribution of longer chains in the range of macrophytes in these settings (Ficken et al., 2000). This dry interval coincides with the highest fatty acid δ^2H values of the record (Figure 4A), which likely reflect the combined effect of increased precipitation δ^2H values and changing vegetation sources (Section 4.1).

Prolonged drought can have devastating effects on crops and food production, leading to food shortages and potential famine (Annamalai et al., 2015; Iese et al., 2021), which can be especially severe for communities relying heavily on horticulture, such as in Melanesia. This can, in turn, impact traditional practices, gardening, hunting, and spiritual beliefs associated with the land and its resources (Mortreux and Barnett, 2009; Smith, 2013), and trigger population movements (Sear et al., 2020). However, the abrupt decline in palmitone is not mirrored in charcoal concentrations, which remained high until ca. 1500 CE, nor by the concentrations of fecal markers, which reached a maximum between 1350–1500 CE (Figure 2). These contrasting records suggest that while the taro crops suffered from the dry conditions or were moved elsewhere, burning continued, indicating that people were still present despite the drier conditions. This could indicate that the drying trend had a negligible impact on local inhabitants, who might have shifted to crops resistant to drier conditions which required land clearance through slash-and-burn, a practice observed elsewhere in the Pacific (Kirch, 1994). This prolonged drought is marked by the large-scale Kuwae eruption (Gao et al., 2006) in 1452 CE, which is associated with major ecosystem shifts in the lake of Emaotul, on the island of Efate, caused by the tephra (Strandberg et al., 2023). However, the absence of tephra in our sediment cores suggests that the eruption did not have a direct impact on west Santo. Fall layers of the Kuwae eruption can be found on Epi, Tongoa, Tongariki, and Efate, hence to the South of Kuwae, which could explain why we do not observe a tephra layer in west Santo (Stern et al., 2023). The population living on the former Kuwae island sought refuge on other islands, especially on Efate, with which they had long standing connections (Garanger, 1972; Robin and Australian Geological Survey Organisation and IAVCEI General Assembly, 1993). Whether people relocated to Santo or there were societal changes related to the eruption remains speculative. Furthermore, the decrease in dryland herbs we observe in Santo after the eruption and the increase in secondary forest would be in contrast with the increase in grass described in Efate (Strandberg et al., 2023). Regional differences and winds might explain the different observations.

4.4 The arrival of Europeans and return to wetter/warmer conditions

Wunavae is located <120 km from Big Bay, where the first Europeans landed in 1606 CE (Figure 1). From historical accounts, we know that the encounter between Europeans and local inhabitants was conflictual and brief, lasting only a few months (Markham, 1904; Kelly, 1966). The impact of European contact

on Pacific Island populations was previously characterized by a substantial decline and, in some cases, near-collapse of these populations (Scarr, 1967; Spriggs, 1997a; Kirch and Rallu, 2007). According to Markham (1904), most of the European crew arriving at Big Bay showed signs of illness. Therefore, the contact with Europeans in Santo could explain the drop in fecal marker and charcoal we observe between 1550–1600 CE, or at least it would have exacerbated the consequences of the prolonged drought (ca. 1400 CE) on humans with the spread of diseases that would have hindered population recovery. However, internal demographic fluctuations could also have played a role, especially in these harsh conditions with absence of water. Various internal migrations took place from inland to the coast in the last two centuries (Pascal, 2020), thus we cannot exclude that over such a long time span (1500–1800 CE) societal changes influenced settlement locations.

After the abrupt decline in human traces (fecal sterols, palmitone, charcoal) observed in the sedimentary records, favorable wetter/warmer conditions characterize the period around 1700 CE. These are signaled by a decrease in n-C_{28} δ^2H values and an increase in MAAT. An increase in precipitation is further evident by an increase in sand content which indicates an increase in erosion further supported by an increase in TOC (Figure 2). The decrease in macrophytes as recorded in the Paq, coupled with an increase in BiSi, would indicate another ecosystem shift possibly driven by higher water levels. The vegetation changes around 1650 CE, with a decline in dryland herbs and an increase in secondary forest, could be indicative of environmental changes linked with a period of increased precipitation but could also be the result of land abandonment. Wetter conditions in Santo would be favorable to the re-establishment of agriculture and settlements, however we do not observe any increase in human traces or other anthropogenic indicators in this period.

4.5 West Santo and the broader climatic context

The environmental changes we have recorded in west Santo took place in the context of two distinct climatic periods that have been observed globally (PAGES 2k Consortium, 2013; Masson-Delmotte et al., 2013; Wanner et al., 2022): the Medieval Climate Anomaly (MCA, ~950–1250 CE) and the LIA. The clearest hydroclimate change recorded in west Santo is the relatively dry period that occurred from ~1400 to ~1650 CE, coinciding with first half of the LIA (Figure 4). The trend towards wetter conditions since that period is consistent with oxygen isotopes from a speleothem from Taurius cave near the southern coast of Santo (Figure 5D; Partin et al., 2013). Hydroclimate changes at any one site in western tropical Pacific may not be indicative of events in the broader region, and within the brief time covered by the instrumental record, precipitation trends throughout the western Pacific are inconsistent (Salinger et al., 2014). In the absence of local factors, however, there are synoptic scale changes that could be expected to cause systematic decreases in precipitation in west Santo: (1) reduced Pacific Walker circulation, similar to the conditions that prevail during El Niño events (Veiga et al., 2005) and (2) equatorward contractions in the mean annual position of the SPCZ, which are
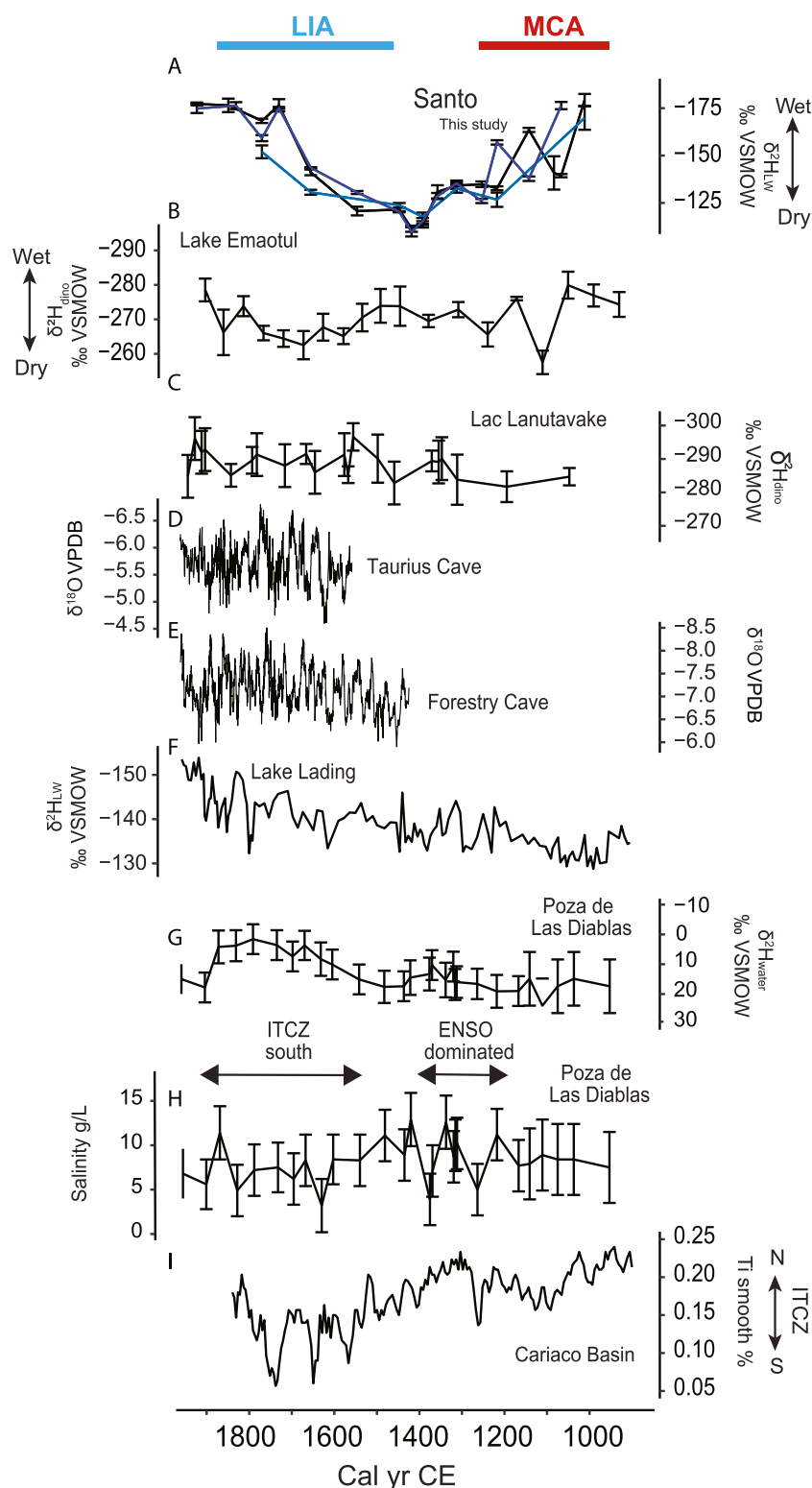
FIGURE 5
Climatic reconstructions for the period 900–2000 CE across the Pacific. **(A)** fatty acids δ^2H_{LW} in west Santo, **(B)** Lake Emaotul (Efate, Vanuatu) $\delta^2H_{dinosterol}$ (Sear et al., 2020), **(C)** Lac Lanutavake $\delta^2H_{dinosterol}$, Uvea, Wallis et Futuna (Maloney et al., 2022) **(D)** $\delta^{18}O$ stalagmite from Taurius Cave, Espiritu Santo (Partin et al., 2013). **(E)** $\delta^{18}O$ stalagmite from Forestry Cave, NW Guadalcanal, Solomon Islands (Maupin et al., 2014) **(F)** Lake Lading δ^2H_{LW}, East Java, Indonesia (Konecky et al., 2013), **(G)** Galápagos Pozo de Las Diablas δ^2H_{water} (Nelson and Sachs, 2016) **(H)** Galapagos Pozo de Las Diablas Salinity (Nelson and Sachs, 2016), **(I)** Cariaco Basin Ti% (Haug et al., 2001). Both $^2H_{water}$ and Salinity from Pozo de Las Diabla were used to infer the dominant climatic influence indicated between both records.

expected to coincide with northward shifts of the ITCZ (Deser et al., 2004; Brown et al., 2020). In isolation, our record of dry conditions in west Santo during the early LIA cannot be attributed to either of these mechanisms, making it important to place our results in the context of other regional records (Figure 5). Most records of climate change of the past millennium from the tropical Pacific are from sites located around the margins of the basin (e.g. Haug et al., 2001; Moy et al., 2002; Higgins et al., 2020; Konecky et al., 2013; Nelson and Sachs, 2016; Jiang et al., 2023; Prohaska et al., 2023), with relatively few records available within the core of the SPCZ. High resolution records from within the core SPCZ are available from speleothems (Partin et al., 2013; Maupin et al., 2014) and corals (Linsley et al., 2008; Tangri et al., 2018; Lawman et al., 2020), but do not span the past millennium. Continuous records of precipitation intensity from lake sediments, such as those from Wallis, Samoa, and southern Vanuatu (Sear et al., 2020; Maloney et al., 2022) and our new west Santo record hence add a western Pacific viewpoint to a growing but still limited body of evidence of the Pacific hydroclimate during the last millennium (Atwood et al., 2021). However, the relatively large age uncertainties in lake sediments (compared to coral and speleothem records) make it difficult to directly compare the timing of hydroclimate changes across sites. Nevertheless, the early LIA dry period in west Santo fits in with a broader pattern of reduced precipitation across the western Pacific during the LIA (Konecky et al., 2013; Partin et al., 2013; Toomey et al., 2016; Sear et al., 2020; Maloney et al., 2022; Prohaska et al., 2023). While a recent analysis of a tree-ring network encompassing the Pacific indicates that there have not been major positional changes in the SPCZ over the past millennium (Higgins et al., 2020), reductions in Pacific Walker Circulation could have decreased precipitation intensity throughout the SPCZ without resulting in a change in the mean annual location of the rain band (Matthews, 2012; Brown et al., 2020).

Importantly, west Santo sediments also demonstrate that sustained changes in rainfall regime are associated with large shifts in the horticultural activities of human communities. Whether changing rainfall patterns are driven by ENSO activity, changes in the mean annual position of SPCZ, or a combination of the two, this impact on human societies demonstrates the critical need to improve our understanding of SPCZ dynamics over time, and to improve our ability to model its behavior, so that local populations can better prepare for future change scenarios.

5 Conclusion

In the Western Pacific, where climatic extremes such as cyclones, droughts, and abrupt climatic shifts are common, the reliance of island societies on the surrounding ecosystems for their livelihoods must have required strategic adaptations to cope with sudden changes. Our records reveal the complex interplay of climate and humans in shaping ancient island environments. Although climatic shifts are evident in the sediment records, these are not reflected in major changes in demography which instead align with the period of first contact with Europeans. This provides a further line of evidence on the resilience of local populations before European contact. A continuity of land use and sustained population is evident from our record prior to European arrival. Demographic

increase characterizes the period around 1000 CE when people started moving inland and expanding horticultural production. The possible anthropogenic origin of the inland reservoirs of Wunavae and Nopovois could be evidence of the water management strategies practiced at the time. A warm and wet interval observed between 1000 and 1400 CE provides the ideal setting for the expansion of agriculture. The drier period around 1400 CE is associated with a prolonged drought which affected the production of taro. However, it was not until 1600 CE that human traces were at a minimum. An increase in precipitation after 1650 CE would have favored agriculture and the growth of taro. However, this coincided with the first European contact, during which new diseases could have been transmitted to the local population. Given the evidence of European impact on other islands in Vanuatu and throughout the Pacific Islands, it is likely that this first contact drove the abrupt demographic decrease observed in our record. Our results reveal details of the history of Melanesia, which emphasize the importance of understanding societal resilience to climate change, particularly in vulnerable environments like island ecosystems.

Data availability statement

The datasets presented in this study can be found in the ETH Zurich Research Collection (Camperio et al., 2025).

Author contributions

GC: Writing – original draft, Software, Data curation, Visualization, Conceptualization, Project administration, Formal Analysis, Writing – review and editing, Methodology, Investigation, Validation. SL: Methodology, Writing – original draft, Formal Analysis, Data curation, Supervision, Investigation, Validation, Conceptualization, Writing – review and editing. MP: Writing – original draft, Supervision, Methodology, Conceptualization, Validation, Investigation, Writing – review and editing, Data curation. CD: Investigation, Writing – review and editing, Validation, Methodology. TS: Validation, Methodology, Writing – review and editing, Writing – original draft, Visualization. EA: Validation, Writing – review and editing, Methodology, Investigation. RL: Writing – review and editing, Methodology, Investigation, Validation. DN: Writing – original draft, Methodology, Validation, Investigation, Writing – review and editing. AD: Writing – review and editing, Methodology. CK: Writing – review and editing, Methodology. ND: Data curation, Validation, Resources, Methodology, Formal Analysis, Conceptualization, Investigation, Writing – review and editing, Funding acquisition, Supervision, Writing – original draft.

Funding

Acknowledgments

Conflict of interest

The authors declare that the research was conducted in the absence of any commercial or financial relationships that could be construed as a potential conflict of interest.

Generative AI statement

The author(s) declare that no Generative AI was used in the creation of this manuscript.

Publisher's note

All claims expressed in this article are solely those of the authors and do not necessarily represent those of their affiliated organizations, or those of the publisher, the editors and the reviewers. Any product that may be evaluated in this article, or claim that may be made by its manufacturer, is not guaranteed or endorsed by the publisher.

Supplementary material

The Supplementary Material for this article can be found online at: https://www.frontiersin.org/articles/10.3389/feart.2025.1613262/full#supplementary-material

References

Allen, M. S. (2006). New ideas about late Holocene climate variability in the Central Pacific. *Curr. Anthropol.* 47 (3), 521–535. doi:10.1086/504168

Anderson, A., Chappell, J., Gagan, M., and Grove, R. (2006). Prehistoric maritime migration in the Pacific Islands: an hypothesis of ENSO forcing. *Holocene* 16 (1), 1–6. doi:10.1191/0959683606hl901ft

Annamalai, H., Keener, V., Widlansky, M. J., and Hafner, J. (2015). *El Niño strengthens in the pacific: preparing for the impacts of drought.* (Honolulu, HI: East–West Center), 2–10.

Atwood, A. R., Battisti, D. S., Wu, E., Frierson, D. M. W., and Sachs, J. P. (2021). Data-model comparisons of tropical hydroclimate changes over the common era. *Paleoceanogr. Paleoclimatology* 36 (7), e2020PA003934. doi:10.1029/2020pa003934

Baan, J., Holloway-Phillips, M., Nelson, D. B., de Vos, J. M., and Kahmen, A. (2025). Phylogenetic and biochemical drivers of plant species variation in organic compound hydrogen stable isotopes: novel mechanistic constraints. *New Phytol.* 246, 113–130. doi:10.1111/nph.20430

Baan, J., Holloway-Phillips, M., Nelson, D. B., and Kahmen, A. (2023). The metabolic sensitivity of hydrogen isotope fractionation differs between plant compounds. *Phytochemistry* 207, 113563. doi:10.1016/j.phytochem.2022.113563

Bayliss-Smith, T., Prebble, M., and Manebosa, S. (2019). "Saltwater and bush in New Georgia, Solomon Islands: exchange relations, agricultural intensification and limits to social complexity," in *Archaeologies of Island Melanesia: Current Approaches to Landscapes, Exchange, and Practice*, ed. M. Leclerc, and J. Flexner (Canberra, ACT, Australia: ANU Press), 32–55.

Bedford, S., Siméoni, P., and Lebot, V. (2018). The anthropogenic transformation of an island landscape: evidence for agricultural development revealed by LiDAR on the island of Efate, Central Vanuatu, South-West Pacific. *Archaeol. Ocean.* 53 (1), 1–14. doi:10.1002/arco.5137

Bedford, S., and Spriggs, M. (2008). Northern Vanuatu as a Pacific crossroads: the archaeology of discovery, interaction, and the emergence of the ethnographic present. *Asian Perspect.* 47, 95–120. doi:10.1353/asi.2008.0003

Bedford, S., and Spriggs, M. (2018). "The archaeology of Vanuatu: 3,000 years of history across Islands of ash and coral," in *The Oxford Handbook of Prehistoric Oceania*, ed. E. E. Cochrane, and T. L. Hunt (Oxford, United Kingdom: Oxford University Press).

Berrocal, M. C., and Sand, C. (2021). A question of impact: did we underestimate the consequences of the sixteenth and seventeenth centuries period of early European exploration in the Pacific? *J. Isl. Coast. Archaeol.* 16 (2–4), 231–260. doi:10.1080/15564894.2019.1679292

Bethell, P. H., Goad, L. J., Evershed, R. P., and Ottaway, J. (1994). The study of molecular markers of human activity: the use of coprostanol in the soil as an indicator of human faecal material. *J. Archaeol. Sci.* 21 (5), 619–632. doi:10.1006/jasc.1994.1061

Blaauw, M., and Christen, J. A. (2011). Flexible paleoclimate age-depth models using an autoregressive gamma process. *Bayesian Anal.* 6(3), 457–474. doi:10.1214/11-ba618

Bouchet, P., Le Guyader, H., and Pascal, O. (2011). *The natural history of Santo* (Paris, France: Muséum d'Histoire naturelle), 421–431.

Brown, J. R., Lengaigne, M., Lintner, B. R., Widlansky, M. J., van Der Wiel, K., Dutheil, C., et al. (2020). South Pacific convergence zone dynamics, variability and impacts in a changing climate. *Nat. Rev. Earth Environ.* 1 (10), 530–543. doi:10.1038/s43017-020-0078-2

Bull, I. D., Elhmmali, M. M., Roberts, D. J., and Evershed, R. P. (2003). The application of steroidal biomarkers to track the abandonment of a Roman wastewater course at the Agora (Athens, Greece). *Archaeometry* 45 (1), 149–161. doi:10.1111/1475-4754.00101

Camperio, G., Ladd, S. N., Prebble, M., De Jonge, C., Schneider, T., Argiriadis, E., et al. (2025). Data from: Human-climate-environment interactions in Espiritu Santo, Vanuatu during the past millennium. *ETH Zurich Research Collection.* doi:10.3929/ethz-b-000743606

Camperio, G., Ladd, S. N., Prebble, M., Lloren, R., Argiriadis, E., Nelson, D. B., et al. (2024). Sedimentary biomarkers of human presence and taro cultivation reveal early horticulture in Remote Oceania. *Commun. Earth Environ.* 5 (1), 667. doi:10.1038/s43247-024-01831-8

Camperio, G. (2024). Sedimentary biomarkers reveal the legacy of human-climate interactions in Vanuatu. Doctoral dissertation. ETH Zurich.

Cashman, K., and Rust, A. (2016). "Introduction: part 2: volcanic ash: generation and spatial variations," in *Volcanic Ash: Hazard Observation* (Amsterdam, Netherlands: Elsevier Inc), 5–22.

Cochrane, E. E., Quintus, S., Prebble, M., Tautunu, T. I., Autufuga, D., Laumea, M., et al. (2024). Collective action problems led to the cultural transformation of Sāmoa 800 years ago. *Plos one* 19 (6), e0304850. doi:10.1371/journal.pone.0304850

Combettes, C., Sémah, A.-M., and Wirrmann, D. (2015). High-resolution pollen record from Efate Island, Central Vanuatu: highlighting climatic and human influences on Late Holocene vegetation dynamics. *Comptes Rendus Palevol* 14 (4), 251–261. doi:10.1016/j.crpv.2015.02.003

Conley, D. J., and Schelske, C. L. (2001). "Biogenic Silica," in *Tracking Environmental Change Using Lake Sediments: Terrestrial, Algal, and Siliceous Indicators, Vol. 3* (Dordrecht: Kluwer Academic Publishers), 281–293.

Conroy, J. L., Cobb, K. M., and Noone, D. (2013). Comparison of precipitation isotope variability across the tropical Pacific in observations and SWING2 model simulations. *J. Geophys. Res. Atmos.* 118 (11), 5867–5892. doi:10.1002/jgrd.50412

Dansgaard, W. (1964). Stable isotopes in precipitation. *Tellus* 16 (4), 436–468. doi:10.1111/j.2153-3490.1964.tb00181.x

De Jonge, C., Hopmans, E. C., Zell, C. I., Kim, J. H., Schouten, S., and Damsté, J. S. S. (2014). Occurrence and abundance of 6-methyl branched glycerol dialkyl glycerol tetraethers in soils: implications for palaeoclimate reconstruction. *Geochimica Cosmochimica Acta* 141, 97–112. doi:10.1016/j.gca.2014.06.013

Deser, C., Phillips, A. S., and Hurrell, J. W. (2004). Pacific interdecadal climate variability: Linkages between the tropics and the North Pacific during boreal winter since 1900. *J. Clim.* 17 (16), 3109–3124.

Eglinton, G., and Hamilton, R. J. (1967). Leaf epicuticular waxes: the waxy outer surfaces of most plants display a wide diversity of fine structure and chemical constituents. *Science* 156 (3780), 1322–1335. doi:10.1126/science.156.3780.1322

Fang, J., Wu, F., Xiong, Y., Li, F., Du, X., An, D., et al. (2014). Source characterization of sedimentary organic matter using molecular and stable carbon isotopic composition of n-alkanes and fatty acids in sediment core from Lake Dianchi, China. *Sci. Total Environ.* 473, 410–421. doi:10.1016/j.scitotenv.2013.10.066

Ferrand, E. A., Dunning, N. P., Lentz, D. L., and Jones, J. G. (2012). Use of aguadas as water management sources in two Southern Maya lowland sites. *Anc. Mesoam.* 23 (1), 85–101. doi:10.1017/s0956536112000065

Ficken, K. J., Li, B., Swain, D. L., and Eglinton, G. (2000). An n-alkane proxy for the sedimentary input of submerged/floating freshwater aquatic macrophytes. *Org. Geochem.* 31 (7-8), 745–749. doi:10.1016/s0146-6380(00)00081-4

Flexner, J. L. (2014). Historical archaeology, contact, and colonialism in Oceania. *J. Archaeol. Res.* 22, 43–87. doi:10.1007/s10814-013-9067-z

François, A., Franjieh, M., Lacrampe, S., and Schnell, S. (2015). The exceptional linguistic density of Vanuatu. in: *The languages of Vanuatu: unity and diversity*, A. François, S. Lacrampe, M. Franjieh, and S. Schnell, 1–21. Chapter: 1, Publisher: Asia–Pacific Linguistics.

Galipaud, J. C. (2000). The lapita site of Atanoasao, Malo, Vanuatu. *World Archaeol. Bull.* 12, 41–55.

Galipaud, J.-C. (2004). Settlement history and landscape use in Santo, Vanuatu. In A Pacific Odyssey: archaeology and anthropology in the Western Pacific. *Rec Austr Museum* 29. 59–64.

Galipaud, J. C. (2011). "The prehistory of Santo," in *The Natural History of Santo*, ed. P. Bouchet, H. Le Guyader, and O. Pascal (Paris, France: Publications Scientifiques du Muséum, Muséum national d'Histoire naturelle), 469–475.

Galipaud, J.-C., and Walter, A. (1997). *Forêts Insulaires. Rapport intermédiaire du programme: Se Nourrir à Santo*. Port Vila. ORSTOM/APFT.

Gao, C., Robock, A., Self, S., Witter, J. B., Steffenson, J. P., Clausen, H. B., et al. (2006). The 1452 or 1453 A.D. Kuwae eruption signal derived from multiple ice core records: greatest volcanic sulfate event of the past 700 years. *J. Geophys. Res.* 111 (D12), D12107. doi:10.1029/2005jd006710

Gao, L., Zheng, M., Fraser, M., and Huang, Y. (2014). Comparable hydrogen isotopic fractionation of plant leaf wax n-alkanoic acids in arid and humid subtropical ecosystems. *Geochem. Geophys. Geosystems* 15 (2), 361–373. doi:10.1002/2013gc005015

Garanger, J. (1972). *Archéologie des nouvelles hébrides: contribution à la connaissance des ıles du centre, 30*. Paris, France: Publications de La Société Des Océanistes.

Gaven, C., Bernat, M., Jouannic, C., and Fw, T. (1980). Mouvements verticaux des Nouvelles-Hébrides pendant les derniers 120 000 ans. Datation de coraux par la méthode Io-U. *Comptes-Rendus l'Académie Sci.* 290 (D), 175–178.

Gong, X., Xu, Z., Lu, W., Tian, Y., Liu, Y., Wang, Z., et al. (2018). Spatial patterns of leaf carbon, nitrogen, and phosphorus stoichiometry of aquatic macrophytes in the arid zone of northwestern China. *Front. Plant Sci.* 9, 1398. doi:10.3389/fpls.2018.01398

Green, R. C. (1991). "Near and remote Oceania: disestablishing 'Melanesia' in culture history," in *Man and a Half: Essays in Pacific Anthropology and Ethnobiology in Honour of Ralph Bulmer (Memoirs of the Polynesian Society)*, ed. A. Pawley. (Auckland: The Polynesian Society), 491–502.

Håkanson, L., and Jansson, M. (1983). *Principles of Lake Sedimentology*. Berlin: Springer, 316.

Haug, G. H., Hughen, K. A., Sigman, D. M., Peterson, L. C., and Röhl, U. (2001). Southward migration of the intertropical convergence zone through the Holocene. *Science* 293 (5533), 1304–1308. doi:10.1126/science.1059725

Higgins, P. A., Palmer, J. G., Turney, C. S. M., Andersen, M. S., and Cook, E. R. (2020). One thousand three hundred years of variability in the position of the South Pacific convergence zone. *Geophys. Res. Lett.* 47 (17), e2020GL088238. doi:10.1029/2020gl088238

Hirave, P., Nelson, D. B., Glendell, M., and Alewell, C. (2023). Land-use-based freshwater sediment source fingerprinting using hydrogen isotope compositions of long-chain fatty acids. *Sci. Total Environ.* 875, 162638. doi:10.1016/j.scitotenv.2023.162638

Hogg, A. G., Heaton, T. J., Hua, Q., Palmer, J. G., Turney, C. S., Southon, J., et al. (2020). SHCal20 Southern Hemisphere calibration, 0–55,000 years cal BP. *Radiocarbon* 62 (4), 759–778. doi:10.1017/rdc.2020.59

Hope, G., O'Dea, D., and Southern, W. (1999). "Holocene vegetation histories in the Western Pacific: alternative records of human impact," in *Le Pacifique de 5000 à 2000 avant le présent: suppléments à l'histoire d'une colonisation = The Pacific from 5000 to 2000 BP: colonisation and transformations*. Editors G. Jean-Christophe, and I. Lilley (Paris: IRD), 387–404. (Colloques et Séminaires). Conférence Lapita : Le Pacifique de 5000 à 2000 avant le Présent : Suppléments à l'Histoire d'une Colonisation, 3., Port Vila (VAN), 1996/06/31.

Hopmans, E. C., Schouten, S., and Sinninghe Damsté, J. S. (2016). The effect of improved chromatography on GDGT-based palaeoproxies. *Org. Geochem.* 93, 1–6. doi:10.1016/j.orggeochem.2015.12.006

Hua, Q., Turnbull, J. C., Santos, G. M., Rakowski, A. Z., Ancapichún, S., De Pol-Holz, R., et al. (2022). Atmospheric radiocarbon for the period 1950–2019. *Radiocarbon* 64 (4), 723–745. doi:10.1017/rdc.2021.95

Iese, V., Kiem, A. S., Mariner, A., Malsale, P., Tofaeono, T., Kirono, D. G., et al. (2021). Historical and future drought impacts in the Pacific islands and atolls. *Clim. Change* 166 (1), 19. doi:10.1007/s10584-021-03112-1

Jiang, S., Zhou, X., Sachs, J. P., Li, Z., Tu, L., Lin, Y., et al. (2023). The mean state of the tropical Pacific Ocean differed between the medieval warm period and the industrial era. *Commun. Earth Environ.* 4 (1), 74. doi:10.1038/s43247-023-00734-4

Jolly, M. (2009). "The sediment of voyages: remembering Quirós, Bougainville and Cook in Vanuatu," in *Oceanic encounters: Exchange, Desire, Violence*, ed. M. Jolly, S. Tcherkézoff, and D. Tryon (Canberra, ACT: ANU ePress), 57–111.

Jouannic, C., Taylor, F. W., Bloom, A. L., and Bernat, M. (1980). Late Quaternary uplift history from emerged reef terraces on Santo and Malekula Islands, central New Hebrides island arc. *CCOP Sopac Tech. Bull.* 3, 91–108.

Keenan, B., Imfeld, A., Johnston, K., Breckenridge, A., Gélinas, Y., and Douglas, P. M. (2021). Molecular evidence for human population change associated with climate events in the Maya lowlands. *Quat. Sci. Rev.* 258, 106904. doi:10.1016/j.quascirev.2021.106904

Kelly, C. (1966). *La Austrialia del Espíritu Santo: the journal of Fray Martín de Munilla O.F.M. and other documents relating to the voyage of Pedro Fernández de Quirós to the South Sea (1605–1606) and the Franciscan Missionary Plan (1617–1627) (Vol. 2)*. Cambridge: The Hakluyt Society.

Kershaw, A. P., Bush, M. B., Hope, G. S., Weiss, K. F., Goldammer, J. G., and Sanford, R. (1997). "The contribution of humans to past biomass burning in the tropics," in *Sediment records of biomass burning and global change. NATO ASI Series*. Editors J. S. Clark, H. Cachier, J. G. Goldammer, and B. Stocks (Berlin, Heidelberg: Springer), Vol. 51, 413–442. doi:10.1007/978-3-642-59171-6_19

Kilbourne, K. H., Quinn, T. M., Taylor, F. W., Delcroix, T., and Gouriou, Y. (2004). El Niño–Southern Oscillation–related salinity variations recorded in the skeletal geochemistry of a Porites coral from Espiritu Santo, Vanuatu. *Paleoceanography* 19 (4), PA4002. doi:10.1029/2004pa001033

Kirch, P. V. (1994). *The Wet and the Dry: Irrigation and Agricultural Intensification in Polynesia*. Chicago, IL: University of Chicago Press.

Kirch, P. V., and Rallu, J.-L. (2007). *The Growth and Collapse of Pacific Island Societies: Archaeological and Demographic Perspectives*. Honolulu, HI: University of Hawai'i Press.

Konecky, B. L., Russell, J. M., Rodysill, J. R., Vuille, M., Bijaksana, S., and Huang, Y. (2013). Intensification of southwestern Indonesian rainfall over the past millennium. *Geophys. Res. Lett.* 40 (2), 386–391. doi:10.1029/2012gl054331

Krentscher, C., Dubois, N., Camperio, G., Prebble, M., and Ladd, S. N. (2019). Palmitone as a potential species-specific biomarker for the crop plant taro (Colocasia esculenta Schott) on remote Pacific islands. *Org. Geochem.* 132, 1–10. doi:10.1016/j.orggeochem.2019.03.006

Ladd, S. N., Maloney, A. E., Nelson, D. B., Prebble, M., Camperio, G., Sear, D. A., et al. (2021). Leaf wax hydrogen isotopes as a hydroclimate proxy in the tropical Pacific. *J. Geophys. Res. Biogeosciences* 126 (3), e2020JG005891. doi:10.1029/2020jg005891

Lawman, A. E., Partin, J. W., Dee, S. G., Casadio, C. A., Cobb, K. M., and Quinn, T. M. (2020). Developing a coral proxy system model to compare coral and climate model estimates of changes in paleo-ENSO variability. *Paleoceanogr. Paleoclimatol.* 35 (7), e2019PA003836. doi:10.1029/2019pa003836

Linsley, B. K., Zhang, P., Kaplan, A., Howe, S. S., and Wellington, G. M. (2008). Interdecadal-decadal climate variability from multicoral oxygen isotope records in

the South Pacific Convergence Zone region since 1650 A.D. *Paleoceanography* 23 (2), PA2219. doi:10.1029/2007pa001539

Lowe, D. J., and Nelson, C. S. (1983). *Guide to the nature and methods of analysis of the clay fraction of tephras from the South Auckland region, 11. New Zealand.*

Maes, C., and Varillon, D. (2011). "Climatic and oceanic conditions around Santo," in *The Natural History of Santo*, ed. P. Bouchet, H. Le Guyader, and O. Pascal (Paris, France: Publications Scientifiques du Muséum, Muséum national d'Histoire naturelle), 57–61.

Maloney, A. E., Richey, J. N., Nelson, D. B., Hing, S. N., Sear, D. A., Hassall, J. D., et al. (2022). Contrasting Common Era climate and hydrology sensitivities from paired lake sediment dinosterol hydrogen isotope records in the South Pacific convergence zone. *Quat. Sci. Rev.* 281, 107421. doi:10.1016/j.quascirev.2022.107421

Markham, C. (1904). *The voyages of Pedro Fernandez de Quirós, 1595 to 1606 (Vol. 2).* Cambridge: The Hakluyt Society.

Marshall, A. J. (1937). *The Black Musketeers: The Work and Adventures of a Scientist on a South Sea Island at War and in Peace.* London, United Kingdom: William Heinemann Ltd.

Masson-Delmotte, V., Schulz, M., Abe-Ouchi, A., Beer, J., Ganopolski, A., González Rouco, J. F., et al. (2013). "Information from paleoclimate archives," in *Climate change 2013 - the physical science basis. Contribution of working group 1 to the fifth assessment report of the intergovernnmental panel on climate change.* Editors T. F. Stocker, D. Qin, G.-K. Plattner, M. Tignor, S. Allen, J. Boschung, et al. (Cambridge, United Kingdom and New York, NY, USA: Cambridge University Press), 383e464.

Matthews, A. J. (2012). A multiscale framework for the origin and variability of the South Pacific Convergence Zone. *Q. J. R. Meteorological Soc.* 138 (666), 1165–1178. doi:10.1002/qj.1870

Maupin, C. R., Partin, J. W., Shen, C. C., Quinn, T. M., Lin, K., Taylor, F. W., et al. (2014). Persistent decadal-scale rainfall variability in the tropical South Pacific Convergence Zone through the past six centuries. *Clim. Past* 10 (4), 1319–1332. doi:10.5194/cp-10-1319-2014

McFarlin, J. M., Axford, Y., Masterson, A. L., and Osburn, M. R. (2019). Calibration of modern sedimentary δ2H plant wax-water relationships in Greenland lakes. *Quat. Sci. Rev.* 225, 105978. doi:10.1016/j.quascirev.2019.105978

Meyers, P. A. (1994). Preservation of elemental and isotopic source identification of sedimentary organic matter. *Chem. Geol.* 114 (3-4), 289–302. doi:10.1016/0009-2541(94)90059-0

Meyers, P. A., and Teranes, J. L. (2001). "Sediment organic matter," in *Tracking environmental change using Lake Sediments*. Editors W. Last, and J. P. Smol (Dordrecht: Kluwer Academic Publishers), 240–267.

Montenegro, Á., Callaghan, R. T., and Fitzpatrick, S. M. (2016). Using seafaring simulations and shortest-hop trajectories to model the prehistoric colonization of Remote Oceania. *Proc. Natl. Acad. Sci. U. S. A.* 113 (45), 12685–12690. doi:10.1073/pnas.1612426113

Moore, P. D., Webb, J. A., and Collison, M. E. (1991). *Pollen Analysis (2nd ed.).* Oxford, United Kingdom: Blackwell Scientific Publications.

Moorehead, A. (1987). *The fatal impact: the invasion of the South pacific.* Sydney: Mead and Beckett, 1767–1840.

Mortreux, C., and Barnett, J. (2009). Climate change, migration and adaptation in Funafuti, Tuvalu. *Glob. Environ. Change* 19, 105–112. doi:10.1016/j.gloenvcha.2008.09.006

Moy, C. M., Seltzer, G. O., Rodbell, D. T., and Anderson, D. M. (2002). Variability of El niño/southern oscillation activity at millennial timescales during the Holocene epoch. *Nature* 420 (6912), 162–165. doi:10.1038/nature01194

Mueller-Dombois, D., and Fosberg, F. R. (1998). "Vegetation of the tropical Pacific islands," in *Series ecological studies, 132*. New York: Springer-Verlag New York, Inc.

Nelson, D. B., and Sachs, J. P. (2016). Galápagos hydroclimate of the Common Era from paired microalgal and mangrove biomarker ²H/¹H values. *Proc. Natl. Acad. Sci. U. S. A.* 113 (13), 3476–3481. doi:10.1073/pnas.1516271113

Nogué, S., de Nascimento, L., Froyd, C. A., Wilmshurst, J. M., de Boer, E. J., Coffey, E. E. D., et al. (2017). Island biodiversity conservation needs palaeoecology. *Nat. Ecol. Evol.* 1 (7), 0181. doi:10.1038/s41559-017-0181

Nogué, S., Santos, A. M., Birks, H. J. B., Björck, S., Castilla-Beltrán, A., Connor, S., et al. (2021). The human dimension of biodiversity changes on islands. *Science* 372 (6541), 488–491. doi:10.1126/science.abd6706

Ohlendorf, C., and Sturm, M. (2008). A modified method for biogenic silica determination. *J. Paleolimnol.* 39 (1), 137–142. doi:10.1007/s10933-007-9100-7

PAGES 2k Consortium (2013). Continental-scale temperature variability during the past two millennia. *Nat. Geosci.* 6, 339–346. doi:10.1038/ngeo1797

Partin, J. W., Quinn, T. M., Shen, C. C., Emile-Geay, J., Taylor, F. W., Maupin, C. R., et al. (2013). Multidecadal rainfall variability in South Pacific Convergence Zone as revealed by stalagmite geochemistry. *Geology* 41 (11), 1143–1146. doi:10.1130/g34718.1

Pascal, E. M. (2020). The potters of Espiritu Santo: a socio-historical study of survival and loss of tradition. Doctoral dissertation. The University of Waikato.

Pickett, E. J., Harrison, S. P., Hope, G., Harle, K., Dodson, J. R., Peter Kershaw, A., et al. (2004). Pollen-based reconstructions of biome distributions for Australia, Southeast Asia and the Pacific (SEAPAC region) at 0, 6000 and 18,000 14C yr BP. *J. Biogeogr.* 31 (9), 1381–1444. doi:10.1111/j.1365-2699.2004.01001.x

Pineda, R. (2011). *Vanuatu REDD + demonstration activities: participatory pilot site demarcation and description. Report for SPC/GIZ regional Project "climate protection through forest conservation in pacific countries".* Suva, Fiji: SPC Land Resources Division.

Poynter, J., and Eglinton, G. (1990). "Molecular composition of three sediments from Hole 717C: The Bengal Fan" in *Proceedings of the Ocean Drilling Program: Scientific Results* ed. J. R. Cochran, and D. A. V. Stow (College Station, TX: Ocean Drilling Program), 155–161.

Prohaska, A., Seddon, A. W., Meese, B., Willis, K. J., Chiang, J. C., and Sachse, D. (2023). Abrupt change in tropical Pacific climate mean state during the Little Ice Age. *Commun. Earth Environ.* 4 (1), 227. doi:10.1038/s43247-023-00882-7

Raposeiro, P. M., Hernández, A., Pla-Rabes, S., Gonçalves, V., Bao, R., Sáez, A., et al. (2021). Climate change facilitated the early colonization of the Azores Archipelago during medieval times. *Proc. Natl. Acad. Sci. U. S. A.* 118 (41), e2108236118. doi:10.1073/pnas.2108236118

Reimer, R. W., and Reimer, P. J. (2023). CALIBomb [WWW program]. Available online at: http://calib.org (accessed October 6, 2023).

Richardson, D. C., Holgerson, M. A., Farragher, M. J., Hoffman, K. K., King, K. B., Alfonso, M. B., et al. (2022). A functional definition to distinguish ponds from lakes and wetlands. *Sci. Rep.* 12 (1), 10472. doi:10.1038/s41598-022-14569-0

Risi, C., Bony, S., and Vimeux, F. (2008). Influence of convective processes on the isotopic composition (δ¹⁸O and δD) of precipitation and water vapor in the tropics: 2. Physical interpretation of the amount effect. *J. Geophys. Res. Atmos.* 113 (D19), D19306. doi:10.1029/2008jd009943

Robin, C., and Australian Geological Survey Organisation, and IAVCEI General Assembly (1993). *The geology, volcanology, petrology-geochemistry, and tectonic evolution of the new hebrides island arc.* Vanuatu. IAVCEI, Canberra 1993: Excursion Guide. Australian Geological Survey Organisation.

Sachs, J. P., Sachse, D., Smittenberg, R. H., Zhang, Z., Battisti, D. S., and Golubic, S. (2009). Southward movement of the Pacific intertropical convergence zone AD 1400–1850. *Nat. Geosci.* 2 (7), 519–525. doi:10.1038/ngeo554

Sachse, D., Billault, I., Bowen, G. J., Chikaraishi, Y., Dawson, T. E., Feakins, S. J., et al. (2012). Molecular paleohydrology: interpreting the hydrogen-isotopic composition of lipid biomarkers from photosynthesizing organisms. *Annu. Rev. Earth Planet. Sci.* 40 (1), 221–249. doi:10.1146/annurev-earth-042711-105535

Salinger, M., Renwick, J., and Mullan, B. (2001). Interdecadal pacific oscillation and south Pacific climate. *Int. J. Climatol.* 21, 1705–1721. doi:10.1002/joc.691

Salinger, M. J., McGree, S., Beucher, F., Power, S. B., and Delage, F. (2014). A new index for variations in the position of the South Pacific convergence zone 1910/11–2011/2012. *Clim. Dyn.* 43, 881–892. doi:10.1007/s00382-013-2035-y

Sánchez-Murillo, R., Esquivel-Hernández, G., Birkel, C., Correa, A., Welsh, K., Durán-Quesada, A. M., et al. (2020). Tracing water sources and fluxes in a dynamic tropical environment: from observations to modeling. *Front. Earth Sci.* 8, 571477. doi:10.3389/feart.2020.571477

Sand, C. (2023). *Hécatombe Océanienne: Histoire de la dépopulation des peuples du Pacifique et ses conséquences (XVIe-XXe siècle).* Brest: Au vent des îles.

Scarr, D. (1967). Recruits and recruiters: a portrait of the Pacific Islands labour trade. *J. Pac. Hist.* 2 (1), 5–24. doi:10.1080/00223346708572099

Scholl, M. A., Ingebritsen, S. E., Janik, C. J., and Kauahikaua, J. P. (1996). Use of precipitation and groundwater isotopes to interpret regional hydrology on a tropical volcanic island: Kilauea Volcano area, Hawaii. *Water Resour. Res.* 32 (12), 3525–3537. doi:10.1029/95wr02837

Sear, D. A., Allen, M. S., Hassall, J. D., Maloney, A. E., Langdon, P. G., Morrison, A. E., et al. (2020). Human settlement of East Polynesia earlier, incremental, and coincident with prolonged South Pacific drought. *Proc. Natl. Acad. Sci. U. S. A.* 117 (16), 8813–8819. doi:10.1073/pnas.1920975117

Shineberg, D. (1967). *They came for sandalwood: a study of the sandalwood trade in the South West Pacific, 1830–1865.* Melbourne: Melbourne University Press.

Smith, R. (2013). Should they stay or should they go? A discourse analysis of factors influencing relocation decisions among the outer islands of Tuvalu and Kiribati. *J. N. Z. Pac. Stud.* 1 (1), 23–39. doi:10.1386/nzps.1.1.23_1

Speiser, F. (1913). *Two Years with the Natives in the Western Pacific.* London, United Kingdom: Mills & Boon.

Spriggs, M. (1997a). *The island melanesians.* Oxford: Blackwell.

Spriggs, M. (1997b). "Landscape catastrophe and landscape enhancement: are either or both true in the Pacific," in *Historical ecology in the Pacific Islands: prehistoric environmental and landscape change*, ed. P. V. Kirch, and T. L. Hunt, (New Haven, CT: Yale University Press), 80–104.

Spriggs, M., Addison, D. J., and Matthews, P. (2012). *Irrigated Taro (Colocasia esculenta) in the Indo-Pacific: Biological, Social and Historical Perspectives.* Osaka: National Museum of Ethnology.

Stern, S., Cronin, S., Bedford, S., Ballard, C., Henderson, R., and Yona, S. (2023). Impacts of the mid-15th century eruption at Kuwae Caldera, Vanuatu. Abstract retrieved from EGU General Assembly Conference Abstracts (Accession no. EGU-1789). doi:10.5194/egusphere-egu23-1789

Strandberg, N. A., Sear, D. A., Langdon, P. G., Cronin, S. J., Langdon, C. T., Maloney, A. E., et al. (2023). Island ecosystem responses to the Kuwae eruption and precipitation change over the last 1600 years, Efate, Vanuatu. *Front. Ecol. Evol.* 11, 1087577. doi:10.3389/fevo.2023.1087577

Tangri, N., Dunbar, R. B., Linsley, B. K., and Mucciarone, D. M. (2018). ENSO's shrinking twentieth-century footprint revealed in a half-millennium coral core from the South pacific convergence zone. *Paleoceanogr. Paleoclimatol.* 33 (11), 1136–1150. doi:10.1029/2017pa003310

Taylor, F. W. (1992). Quaternary vertical tectonics of the central new Hebrides island arc. *Proc. Ocean. Drill. Program Initial. Rep.* 134, 33–42.

Tenzer, G. E., Meyers, P. A., Robbins, J. A., Eadie, B. J., Morehead, N. R., and Lansing, M. B. (1999). Sedimentary organic matter record of recent environmental changes in the St. Marys River ecosystem, Michigan–Ontario border. *Org. Geochem.* 30 (2-3), 133–146. doi:10.1016/s0146-6380(98)00209-5

Terry, J. P. (2011). "Hydrology and fluvial geomorphology," in *The natural history of Santo*. Paris: MNHN, 46–51.

Toomey, M. R., Donnelly, J. P., and Tierney, J. E. (2016). South Pacific hydrologic and cyclone variability during the last 3000 years. *Paleoceanography* 31 (4), 491–504. doi:10.1002/2015pa002870

Tryon, D. T. (1996). "Mae-morae and the languages of Epi (Vanuatu)," in *Oceanic Studies: Proceedings of the First International Conference on Oceanic Llinguistics* (Canberra, ACT: Pacific Linguistics, Research School of Pacific and Asian Studies, Australian National University), 305–318.

Tzerikiantz, F. (2006). "Ples blong mi wea? (Où est ma terre ?) Pratiques et discours contemporains autour de la mobilité à l'Ouest de Santo, Vanuatu. Université Aix-Marseille I ED 355 Espaces," in *Cultures, Sociétés Laboratoire d'accueil: CREDO-UMR 6574 (Centre de Recherche et de Documentation sur l'Océanie) Maison Asie Pacifique, Université de Provence*. Marseille: Thèse de Doctorat.

Veiga, J. P., Rao, V. B., and Franchito, S. H. (2005). Heat and moisture budgets of the Walker circulation and associated rainfall anomalies during El Niño events: walker circulation heat and moisture budgets. *Int. J. Climatol. A J. R. Meteorological Soc.* 25 (2), 193–213. doi:10.1002/joc.1115

Wanner, H., Pfister, C., and Neukom, R. (2022). The variable European little ice age. *Quat. Sci. Rev.* 287, 107531. doi:10.1016/j.quascirev.2022.107531

White, A. J., Stevens, L. R., Lorenzi, V., Munoz, S. E., Schroeder, S., Cao, A., et al. (2019). Fecal stanols show simultaneous flooding and seasonal precipitation change correlate with Cahokia's population decline. *Proc. Natl. Acad. Sci. U. S. A.* 116 (12), 5461–5466. doi:10.1073/pnas.1809400116

Wirrmann, D., Galipaud, J. C., Sémah, A. M., and Alcover, J. A. (2011). "Caves as archives," in *The natural history of Santo*. Paris: MNHN, 278–284.

Xia, C., Yu, D., Wang, Z., and Xie, D. (2014). Stoichiometry patterns of leaf carbon, nitrogen and phosphorous in aquatic macrophytes in eastern China. *Ecol. Eng.* 70, 406–413. doi:10.1016/j.ecoleng.2014.06.018

Zhao, B., Russell, J. M., Tsai, V. C., Blaus, A., Parish, M. C., Liang, J., et al. (2023). Evaluating global temperature calibrations for lacustrine branched GDGTs: seasonal variability, paleoclimate implications, and future directions. *Quat. Sci. Rev.* 310, 108124. doi:10.1016/j.quascirev.2023.108124